A posteriori error analysis of an augmented mixed formulation in linear elasticity with mixed and Dirichlet boundary conditions *

Tomás P. Barrios†, Edwin M. Behrens‡, María González§

Abstract

We develop a residual-based a posteriori error analysis for the augmented mixed methods introduced in [17] and [18] for the problem of linear elasticity in the plane. We prove that the proposed a posteriori error estimators are both reliable and efficient. Numerical experiments confirm these theoretical properties and illustrate the ability of the corresponding adaptive algorithms to localize the singularities and large stress regions of the solutions.

Key words: Mixed finite element, augmented formulation, a posteriori error estimator, linear elasticity

Mathematics Subject Classifications (1991): 65N15, 65N30, 65N50, 74B05, 74S05

1 Introduction

Recently, a new stabilized mixed finite element method was presented and analyzed in [17] for the problem of linear elasticity in the plane assuming pure homogeneous Dirichlet boundary conditions and mixed boundary conditions with non-homogeneous Neumann data. This approach was extended to the case of pure non-homogeneous Dirichlet boundary conditions in the subsequent work [18].

*This research was partially supported by CONICYT-Chile through the FONDECYT grants 11060014 and 11070085, by the Dirección de Investigación of the Universidad Católica de la Santísima Concepción, and by MEC and Xunta de Galicia through projects MTM2007-67596-C02-01 and PGIDIT06PXIB105230PR, respectively.

†Departamento de Matemática y Física Aplicadas, Universidad Católica de la Santísima Concepción, Casilla 297, Concepción, Chile, email: tomas@ucsc.cl

‡Departamento de Ingeniería Civil, Universidad Católica de la Santísima Concepción, Casilla 297, Concepción, Chile, email: ebehrens@ucsc.cl

§Departamento de Matemáticas, Universidad de A Coruña, Campus de Elviña s/n, 15071, A Coruña, Spain, email: mgtaboad@udc.es

The augmented formulations proposed in [17, 18] rely on the mixed method of Hellinger and Reissner that provides simultaneous approximations of the displacement $\mathbf{u}$ and the stress tensor $\boldsymbol{\sigma}$. The symmetry of $\boldsymbol{\sigma}$ is imposed weakly through the use of a Lagrange multiplier, which enters the system as a new variable that can be interpreted as the rotation $\boldsymbol{\gamma} := \frac{1}{2}(\nabla\mathbf{u} - (\nabla\mathbf{u})^{\mathtt{t}})$ (see [1, 23]). When mixed boundary conditions are considered, the essential one (Neumann) is also imposed weakly, which yields the introduction of the trace of the displacement on the Neumann boundary as a Lagrange multiplier (see [6]).

Although the usual dual-mixed variational formulations satisfy the hypotheses of the Babuška-Brezzi theory, it is difficult to derive explicit finite element subspaces yielding stable discrete schemes. In particular, when mixed boundary conditions with non-homogeneous Neumann data are imposed, the PEERS elements can be applied but they yield a non-conforming Galerkin scheme. This was one of the main motivations to introduce the augmented formulation from [17].

The approach there is based on the introduction of suitable Galerkin least-squares terms that arise from the constitutive and equilibrium equations, and from the relation defining the rotation in terms of the displacement. In [18], besides these Galerkin least-squares terms, a consistency term related with the non-homogeneous Dirichlet boundary condition is added. In the case of pure Dirichlet boundary conditions, the bilinear form of the augmented formulation is bounded and coercive on the whole space and hence, the associated Galerkin scheme is well-posed for *any* finite element subspace. Thus, it is possible to use as finite element subspaces some non-feasible choices for the usual (non-augmented) dual-mixed formulation. In particular, it is possible to employ Raviart-Thomas elements of lowest order to approximate the stress tensor, continuous piecewise linear elements for the displacement, and piecewise constants for the rotation. In the case of mixed boundary conditions, the trace of the displacement on the Neumann boundary can be approximated by continuous piecewise linear elements on an independent partition of that boundary whose mesh size needs to satisfy a compatibility condition with the mesh size of the triangulation of the domain.

As pointed out in [17, 18], when uniform triangulations are used the mixed finite element schemes proposed there are cheaper than the classical PEERS and BDM elements. More precisely, in the lowest order case the total number of unknowns (dof) for the augmented scheme behaves asymptotically as $5\bar{m}$, where $\bar{m}$ is the number of triangles in the triangulation; for PEERS and BDM (with a static condensation process), the total number of dof behaves asymptotically as $7.5\bar{m}$ and $9\bar{m}$, respectively (see section 5 in [8] for more details). On the other hand, the lowest order symmetric mixed finite element proposed recently in [5] consists of piecewise linear displacements and piecewise quadratic stresses augmented with some cubic functions and involves 30 dof per triangle; the total number of unknowns in this case behaves asymptotically as $11.5\bar{m}$. More recently, a mixed finite element method with weakly imposed symmetry has been proposed in [2]. In the lowest order case, the stresses are approximated by the Cartesian product of two copies of the BDM finite element space and the displacements and rotations are approximated by piecewise constants; the total number of dof in this case behaves asymptotically as $9\bar{m}$. A reduced element involving asymptotically $7.5\bar{m}$ dof was also presented in [2]. We must also mention that the approach in [17, 18] was recently extended in [20] to the 3D linear elasticity problem with pure Dirichlet boundary conditions. This approach seems to be advantageous as compared with the mixed finite element method from [4] (see [20] for more details).

Motivated by the competitive character of the augmented scheme introduced in [17], an a posteriori error analysis of residual type was developed in [8] in the case of pure homogeneous Dirichlet boundary conditions. In this paper, we extend the analysis in [8] to the augmented schemes introduced in [17] for the case of mixed boundary conditions and in [18] for non-homogeneous Dirichlet boundary conditions.

The rest of the paper is organized as follows. In section 2, we recall the continuous and discrete augmented formulations proposed in [17] for problem (2.1). We develop a residual based a posteriori error analysis and show that the a posteriori error estimator is both reliable and efficient. Then, in section 3, we recall from [18] the augmented variational and discrete schemes proposed in the case of non-homogeneous Dirichlet boundary conditions, and deduce an a posteriori error estimator of residual type which is shown to be both reliable and efficient. Finally, in section 4 we provide several numerical results that illustrate the performance of the augmented Galerkin schemes and confirm the theoretical properties of the a posteriori error estimators introduced in this paper. Moreover, numerical experiments show that the adaptive algorithms based on these a posteriori error estimators are able to localize the singularities and large stress regions of the solutions.

Notation and preliminary results. Given any Hilbert space H, we denote by H^2 and $H^{2\times 2}$, respectively, the spaces of vectors and square tensors of order 2 with entries in H. In particular, given $\boldsymbol{\tau} := (\tau_{ij})$ and $\boldsymbol{\zeta} := (\zeta_{ij}) \in \mathbb{R}^{2\times 2}$, we denote $\boldsymbol{\tau}^{\mathtt{t}} := (\tau_{ji})$, $\operatorname{tr}(\boldsymbol{\tau}) := \tau_{11} + \tau_{22}$ and $\boldsymbol{\tau} : \boldsymbol{\zeta} := \sum_{i,j=1}^{2} \tau_{ij}\, \zeta_{ij}$. In addition, given differentiable scalar, vector and tensor fields, ϕ, $\mathbf{v} = (v_i) \in \mathbb{R}^2$ and $\boldsymbol{\tau} := (\tau_{ij}) \in \mathbb{R}^{2\times 2}$,

$$\mathbf{curl}(\phi) := \begin{pmatrix} -\frac{\partial \phi}{\partial x_2} \\ \frac{\partial \phi}{\partial x_1} \end{pmatrix} \quad \underline{\mathbf{curl}}(\mathbf{v}) := \begin{pmatrix} \mathbf{curl}(v_1)^{\mathtt{t}} \\ \mathbf{curl}(v_2)^{\mathtt{t}} \end{pmatrix} \quad \mathbf{curl}(\boldsymbol{\tau}) := \begin{pmatrix} \frac{\partial \tau_{12}}{\partial x_1} - \frac{\partial \tau_{11}}{\partial x_2} \\ \frac{\partial \tau_{22}}{\partial x_1} - \frac{\partial \tau_{21}}{\partial x_2} \end{pmatrix}.$$

Let $\Omega \subset \mathbb{R}^2$ be a bounded and simply connected domain with polygonal boundary Γ, and let Γ_D and Γ_N be two disjoint subsets of Γ such that Γ_D has positive measure and $\Gamma = \bar{\Gamma}_D \cup \bar{\Gamma}_N$. We use the standard terminology for Sobolev spaces and norms. We denote $H^1_{\Gamma_D}(\Omega) := \{\, v \in H^1(\Omega) \,:\, v = 0 \text{ on } \Gamma_D \,\}$, $H(\mathbf{div};\Omega) := \{\boldsymbol{\tau} \in [L^2(\Omega)]^{2\times 2} \,:\, \mathbf{div}(\boldsymbol{\tau}) \in [L^2(\Omega)]^2 \,\}$ and $[L^2(\Omega)]^{2\times 2}_{\mathtt{skew}} := \{\, \boldsymbol{\eta} \in [L^2(\Omega)]^{2\times 2} \,:\, \boldsymbol{\eta} + \boldsymbol{\eta}^{\mathtt{t}} = \mathbf{0} \,\}$. We recall that $[H^{-1/2}(\Gamma_N)]^2$ is the dual of the space $[H^{1/2}_{00}(\Gamma_N)]^2 := \{\mathbf{v}|_{\Gamma_N} \,:\, \mathbf{v} \in [H^1(\Omega)]^2 ,\ \mathbf{v} = \mathbf{0} \text{ on } \Gamma_D\}$ and denote by $\langle \cdot, \cdot \rangle_{\Gamma_N}$ the associated duality pairing with respect to the $[L^2(\Gamma_N)]^2$-inner product; cf. [22].

Let $\{\mathcal{T}_h\}_{h>0}$ be a regular family of triangulations of $\bar{\Omega}$. We assume that for all $h > 0$, $\bar{\Omega} = \cup\{\, T \,:\, T \in \mathcal{T}_h \,\}$ and each point in $\bar{\Gamma}_D \cap \bar{\Gamma}_N$ is a vertex of $\mathcal{T}_h$. Given a triangle $T \in \mathcal{T}_h$, we denote by h_T its diameter and define the mesh size $h := \max\{\, h_T \,:\, T \in \mathcal{T}_h \,\}$; we denote by $E(T)$ the set of the edges of T, and by E_h the set of all the edges of triangles in the triangulation $\mathcal{T}_h$. Then, we can write $E_h = E_h(\Omega) \cup E_h(\Gamma_D) \cup E_h(\Gamma_N)$, where $E_h(S) := \{e \in E_h \,:\, e \subseteq S\}$ for $S \subset \mathbb{R}^2$. Given an edge $e \in E_h$, we denote by h_e the length of e. In addition, given an integer $\ell \geq 0$ and a subset S of $\mathbb{R}^2$, we denote by $\mathcal{P}_\ell(S)$ the space of polynomials in two variables defined in S of total degree at most ℓ, and for each $T \in \mathcal{T}_h$, we define the local Raviart-Thomas space of order zero $\mathcal{RT}_0(T) := \text{span}\,\{\, \mathbf{e}_1,\, \mathbf{e}_2,\, \mathbf{x}\} \subseteq [\mathcal{P}_1(T)]^2$, where $\{\mathbf{e}_1, \mathbf{e}_2\}$ is the canonical basis of $\mathbb{R}^2$ and $\mathbf{x}$ is a generic vector of $\mathbb{R}^2$. Finally, we use C or c, with or without subscripts, to denote generic constants, independent of the discretization parameters, which may take different values at different occurrences.

In order to prove the reliability of the a posteriori error estimators, we will make use of the well-known Clément interpolation operator, $I_h : H^1(\Omega) \to X_h$ (see [15]), where X_h is the space of continuous, piecewise linear functions on $\mathcal{T}_h$. We recall that I_h is defined so that $I_h(v) \in X_h \cap H^1_{\Gamma_D}(\Omega)$ for all $v \in H^1_{\Gamma_D}(\Omega)$. The standard local approximation properties stated in the following lemma are proved in [15].

Lemma 1.1 *There exist positive constants c_1, c_2, independent of h, such that for all $\varphi \in H^1(\Omega)$ there hold*

$$\|\varphi - I_h(\varphi)\|_{L^2(T)} \,\leq\, c_1\, h_T\, \|\varphi\|_{H^1(\Delta(T))} \quad \forall\, T \,\in\, \mathcal{T}_h$$
$$\|\varphi - I_h(\varphi)\|_{L^2(e)} \,\leq\, c_2\, h_e^{1/2}\, \|\varphi\|_{H^1(\Delta(e))} \quad \forall\, e \,\in\, E_h$$

where $\Delta(T) := \cup\{T' \in \mathcal{T}_h \,:\, T' \cap T \neq \emptyset\}$ and $\Delta(e) := \cup\{T' \in \mathcal{T}_h \,:\, T' \cap e \neq \emptyset\}$.

To prove the efficiency of the a posteriori error estimators, we proceed as in [11] and [12], and use inverse inequalities and the localization technique introduced in [25], which is based on triangle-bubble and edge-bubble functions. Given $T \in \mathcal{T}_h$ and $e \in E(T)$, we let ψ_T and ψ_e be the usual triangle-bubble and edge-bubble functions (see (1.5) and (1.6) in [25], respectively). In particular, $\psi_T \in \mathcal{P}_3(T)$, $\text{supp}(\psi_T) \subset T$, $\psi_T = 0$ on ∂T, and $0 \leq \psi_T \leq 1$ in T. Similarly, $\psi_e|_T \in \mathcal{P}_2(T)$, $\text{supp}(\psi_e) \subseteq \omega_e := \cup\{T' \in \mathcal{T}_h \,:\, e \in E(T')\}$, $\psi_e = 0$ on $\partial T \backslash e$, and $0 \leq \psi_e \leq 1$ in ω_e. We also recall from [24] that, given $k \in \mathbb{N}$, there exists an extension operator $L : C(e) \to C(T)$ such that for all $p \in \mathcal{P}_k(e)$, $L(p) \in \mathcal{P}_k(T)$ and $L(p)|_e = p$. In the following lemma we collect some additional properties of ψ_T, ψ_e and L.

Lemma 1.2 *Let $k \in \mathbb{N}$. For any triangle T, there exist positive constants c_1, c_2, c_3 and c_4, depending only on k and the shape of T, such that for all $q \in \mathcal{P}_k(T)$ and $p \in \mathcal{P}_k(e)$, there hold*

$$\|\psi_T\, q\|_{L^2(T)} \,\leq\, \|q\|_{L^2(T)} \,\leq\, c_1\, \|\psi_T^{1/2}\, q\|_{L^2(T)}\,, \tag{1.1}$$

$$\|\psi_e\, p\|_{L^2(e)} \;\le\; \|p\|_{L^2(e)} \;\le\; c_2\, \|\psi_e^{1/2}\, p\|_{L^2(e)}\,, \tag{1.2}$$

$$c_4\, h_e^{1/2}\, \|p\|_{L^2(e)} \;\le\; \|\psi_e^{1/2}\, L(p)\|_{L^2(T)} \;\le\; c_3\, h_e^{1/2}\, \|p\|_{L^2(e)}\,. \tag{1.3}$$

Proof. See Lemma 4.1 in [24]. □

The following inverse estimate will also be used.

Lemma 1.3 *Let $k \in \mathbb{N}$. Let $l, m \in \mathbb{N}$ such that $l \le m$. Then, for any triangle T, there exists $c > 0$, depending only on k, l, m and the shape of T, such that*

$$|q|_{H^m(T)} \;\le\; c\, h_T^{l-m}\, |q|_{H^l(T)} \quad \forall\, q \in \mathcal{P}_k(T)\,.$$

Proof. See Theorem 3.2.6 in [14]. □

2 The case of mixed boundary conditions

In this section, we obtain an a posteriori error estimator of residual type for the augmented mixed finite element scheme introduced in [17] for the problem of linear elasticity with mixed boundary conditions. More precisely, given a volume force $\mathbf{f} \in [L^2(\Omega)]^2$ and a traction $\mathbf{g} \in [H^{-1/2}(\Gamma_N)]^2$, we consider the problem of determining the displacement vector field $\mathbf{u}$ and the symmetric stress tensor field $\boldsymbol{\sigma}$ of a linear elastic material occupying the region Ω:

$$\left\{ \begin{array}{rcll} \boldsymbol{\sigma} &=& \mathcal{C}\, \boldsymbol{\varepsilon}(\mathbf{u}) & \text{in } \Omega \\ -\mathbf{div}(\boldsymbol{\sigma}) &=& \mathbf{f} & \text{in } \Omega \\ \mathbf{u} &=& \mathbf{0} & \text{on } \Gamma_D \\ \boldsymbol{\sigma}\mathbf{n} &=& \mathbf{g} & \text{on } \Gamma_N \end{array} \right. \tag{2.1}$$

where $\mathcal{C}$ is the elasticity tensor determined by Hooke's law, that is,

$$\mathcal{C}\, \boldsymbol{\zeta} \;:=\; \lambda\, \mathrm{tr}(\boldsymbol{\zeta})\, \mathbf{I} \;+\; 2\, \mu\, \boldsymbol{\zeta} \qquad \forall\, \boldsymbol{\zeta} \in [L^2(\Omega)]^{2\times 2}\,, \tag{2.2}$$

with $\mathbf{I}$ being the identity matrix of $\mathbb{R}^{2\times 2}$ and $\lambda,\, \mu > 0$ the Lamé constants; $\boldsymbol{\varepsilon}(\mathbf{u}) := \frac{1}{2}\,(\nabla\mathbf{u} + (\nabla\mathbf{u})^{\mathtt{t}})$ is the strain tensor of small deformations and $\mathbf{n}$ is the unit outward normal to Γ. In the next two subsections, we recall the augmented variational and discrete formulations proposed in [17] to solve problem (2.1).

2.1 The augmented variational formulation

Let κ_1, κ_2 and κ_3 be positive parameters. The augmented variational formulation proposed in [17] for problem (2.1) reads: find $((\boldsymbol{\sigma}, \mathbf{u}, \gamma), \boldsymbol{\xi}) \in \mathbf{H} \times \mathbf{Q}$ such that for any $((\boldsymbol{\tau}, \mathbf{v}, \boldsymbol{\eta}), \boldsymbol{\chi}) \in \mathbf{H} \times \mathbf{Q}$ there hold

$$\left\{ \begin{array}{rcl} A((\boldsymbol{\sigma}, \mathbf{u}, \gamma), (\boldsymbol{\tau}, \mathbf{v}, \boldsymbol{\eta})) \;+\; B((\boldsymbol{\tau}, \mathbf{v}, \boldsymbol{\eta}), \boldsymbol{\xi}) &=& F(\boldsymbol{\tau}, \mathbf{v}, \boldsymbol{\eta}), \\ B((\boldsymbol{\sigma}, \mathbf{u}, \gamma), \boldsymbol{\chi}) &=& G(\boldsymbol{\chi}), \end{array} \right. \tag{2.3}$$

where $\mathbf{H} := H(\mathbf{div};\Omega) \times [H^1_{\Gamma_D}(\Omega)]^2 \times [L^2(\Omega)]^{2\times 2}_{\tt skew}$, $\mathbf{Q} := [H^{1/2}_{00}(\Gamma_N)]^2$, the bilinear form $A : \mathbf{H}\times\mathbf{H} \to \mathbb{R}$ is given by

$$\begin{aligned}
A((\boldsymbol{\sigma},\mathbf{u},\boldsymbol{\gamma}),(\boldsymbol{\tau},\mathbf{v},\boldsymbol{\eta})) &:= \int_\Omega \mathcal{C}^{-1}\boldsymbol{\sigma} : \boldsymbol{\tau} + \int_\Omega \mathbf{u}\cdot\mathbf{div}(\boldsymbol{\tau}) + \int_\Omega \boldsymbol{\tau} : \boldsymbol{\gamma} - \int_\Omega \mathbf{v}\cdot\mathbf{div}(\boldsymbol{\sigma}) \\
&- \int_\Omega \boldsymbol{\sigma} : \boldsymbol{\eta} + \kappa_1 \int_\Omega \left(\boldsymbol{\varepsilon}(\mathbf{u}) - \mathcal{C}^{-1}\boldsymbol{\sigma}\right) : \left(\boldsymbol{\varepsilon}(\mathbf{v}) + \mathcal{C}^{-1}\boldsymbol{\tau}\right) + \kappa_2 \int_\Omega \mathbf{div}(\boldsymbol{\sigma})\cdot\mathbf{div}(\boldsymbol{\tau}) \\
&+ \kappa_3 \int_\Omega \left(\boldsymbol{\gamma} - \frac{1}{2}(\nabla\mathbf{u} - (\nabla\mathbf{u})^{\tt t})\right) : \left(\boldsymbol{\eta} + \frac{1}{2}(\nabla\mathbf{v} - (\nabla\mathbf{v})^{\tt t})\right),
\end{aligned} \tag{2.4}$$

with $\mathcal{C}^{-1}\boldsymbol{\zeta} := \frac{1}{2\mu}\boldsymbol{\zeta} - \frac{\lambda}{4\mu(\lambda+\mu)}\operatorname{tr}(\boldsymbol{\zeta})\,\mathbf{I}$, $B((\boldsymbol{\tau},\mathbf{v},\boldsymbol{\eta}),\boldsymbol{\chi}) := \langle\boldsymbol{\tau}\mathbf{n},\boldsymbol{\chi}\rangle_{\Gamma_N}$, for all $(\boldsymbol{\tau},\mathbf{v},\boldsymbol{\eta}) \in \mathbf{H}$ and $\boldsymbol{\chi}\in\mathbf{Q}$, and the linear functionals $F : \mathbf{H}\to\mathbb{R}$ and $G : \mathbf{Q}\to\mathbb{R}$ are given by

$$F(\boldsymbol{\tau},\mathbf{v},\boldsymbol{\eta}) := \int_\Omega \mathbf{f}\cdot(\,\mathbf{v} - \kappa_2\,\mathbf{div}(\boldsymbol{\tau})\,) \qquad G(\boldsymbol{\chi}) := \langle\mathbf{g},\boldsymbol{\chi}\rangle_{\Gamma_N}. \tag{2.5}$$

The consistency of the augmented formulation (2.3) with the dual-mixed formulation considered in [17] was studied there. The idea is to choose the parameters κ_1, κ_2 and κ_3 independent of λ and such that (2.3) satisfies the hypotheses of the Babuška-Brezzi theory. In what follows, we consider the following inner product in $\mathbf{H}$:

$$\langle(\boldsymbol{\sigma},\mathbf{u},\boldsymbol{\gamma}),(\boldsymbol{\tau},\mathbf{v},\boldsymbol{\eta})\rangle_{\mathbf{H}} := (\boldsymbol{\sigma},\boldsymbol{\tau})_{H(\mathbf{div};\Omega)} + (\mathbf{u},\mathbf{v})_{[H^1(\Omega)]^2} + (\boldsymbol{\gamma},\boldsymbol{\eta})_{[L^2(\Omega)]^{2\times2}}$$

and denote the induced norm by $||\cdot||_{\mathbf{H}}$. We remark that the null space of B is given by

$$\mathbf{V} := \{\,(\boldsymbol{\tau},\mathbf{v},\boldsymbol{\eta}) \in \mathbf{H} : \boldsymbol{\tau}\mathbf{n} = \mathbf{0} \text{ on } \Gamma_N\,\}.$$

The following properties and results were proved in [17].

Theorem 2.1 *Assume that $(\kappa_1,\kappa_2,\kappa_3)$ is independent of λ and such that $0<\kappa_1<2\mu$, $0<\kappa_2$ and $0<\kappa_3<\kappa_1\dfrac{k_D}{1-k_D}$, where $k_D\in(0,1)$ is the constant of Korn's first inequality. Then, there exist positive constants M, α and β, independent of λ, such that*

$$\begin{aligned}
|A((\boldsymbol{\sigma},\mathbf{u},\boldsymbol{\gamma}),(\boldsymbol{\tau},\mathbf{v},\boldsymbol{\eta}))| &\le M\,\|(\boldsymbol{\sigma},\mathbf{u},\boldsymbol{\gamma})\|_{\mathbf{H}}\,\|(\boldsymbol{\tau},\mathbf{v},\boldsymbol{\eta})\|_{\mathbf{H}} \qquad \forall\,(\boldsymbol{\sigma},\mathbf{u},\boldsymbol{\gamma}),\,(\boldsymbol{\tau},\mathbf{v},\boldsymbol{\eta})\in\mathbf{H}, \\
A((\boldsymbol{\tau},\mathbf{v},\boldsymbol{\eta}),(\boldsymbol{\tau},\mathbf{v},\boldsymbol{\eta})) &\ge \alpha\,\|(\boldsymbol{\tau},\mathbf{v},\boldsymbol{\eta})\|^2_{\mathbf{H}} \qquad \forall\,(\boldsymbol{\tau},\mathbf{v},\boldsymbol{\eta})\in\mathbf{V}, \\
\sup_{\mathbf{0}\neq\boldsymbol{\tau}\in H_0} \frac{\langle\boldsymbol{\tau}\mathbf{n},\boldsymbol{\chi}\rangle_{\Gamma_N}}{\|\boldsymbol{\tau}\|_{H(\mathbf{div};\Omega)}} &\ge \beta\,\|\boldsymbol{\chi}\|_{\mathbf{Q}} \qquad \forall\,\boldsymbol{\chi}\in\mathbf{Q},
\end{aligned} \tag{2.6}$$

where $H_0 = \{\boldsymbol{\tau}\in H(\mathbf{div};\Omega) : \boldsymbol{\tau} = \boldsymbol{\tau}^{\tt t}, \quad \mathbf{div}(\boldsymbol{\tau}) = \mathbf{0} \quad \text{in } \Omega\}$. Moreover, the augmented variational formulation (2.3) has a unique solution $((\boldsymbol{\sigma},\mathbf{u},\boldsymbol{\gamma}),\boldsymbol{\xi}) \in \mathbf{H}\times\mathbf{Q}$, with $\boldsymbol{\xi} = -\mathbf{u}|_{\Gamma_N}$, and there exists a positive constant C, independent of λ, such that

$$\|((\boldsymbol{\sigma},\mathbf{u},\boldsymbol{\gamma}),\boldsymbol{\xi})\|_{\mathbf{H}\times\mathbf{Q}} \le C\left(\|\mathbf{f}\|_{[L^2(\Omega)]^2} + \|\mathbf{g}\|_{[H^{-1/2}(\Gamma_N)]^2}\right).$$

Proof. See Theorem 3.3, Lemma 2.3 and Theorem 3.4 in [17]. □

2.2 The augmented discrete scheme

From now on, we assume that κ_1, κ_2 and κ_3 satisfy the assumptions of Theorem 2.1. Let h and $\tilde{h}$ be two positive parameters, and let $\mathbf{H}_h$ and $\mathbf{Q}_{\tilde{h}}$ be any finite element subspaces of $\mathbf{H}$ and $\mathbf{Q}$, respectively. Then, a Galerkin scheme associated to the augmented variational formulation (2.3) reads: find $((\boldsymbol{\sigma}_h, \mathbf{u}_h, \boldsymbol{\gamma}_h), \boldsymbol{\xi}_{\tilde{h}}) \in \mathbf{H}_h \times \mathbf{Q}_{\tilde{h}}$ such that for any $((\boldsymbol{\tau}_h, \mathbf{v}_h, \boldsymbol{\eta}_h), \boldsymbol{\chi}_{\tilde{h}}) \in \mathbf{H}_h \times \mathbf{Q}_{\tilde{h}}$ there hold

$$\left\{ \begin{array}{rcl} A((\boldsymbol{\sigma}_h, \mathbf{u}_h, \boldsymbol{\gamma}_h), (\boldsymbol{\tau}_h, \mathbf{v}_h, \boldsymbol{\eta}_h)) + B((\boldsymbol{\tau}_h, \mathbf{v}_h, \boldsymbol{\eta}_h), \boldsymbol{\xi}_{\tilde{h}}) & = & F(\boldsymbol{\tau}_h, \mathbf{v}_h, \boldsymbol{\eta}_h), \\ B((\boldsymbol{\sigma}_h, \mathbf{u}_h, \boldsymbol{\gamma}_h), \boldsymbol{\chi}_{\tilde{h}}) & = & G(\boldsymbol{\chi}_{\tilde{h}}). \end{array} \right. \tag{2.7}$$

As is well-known, the properties of the bilinear form B are not directly transferred to the discrete level and need to be proved for each particular choice of the corresponding finite element subspaces. We recall next the simplest choice of stable finite element subspaces $\mathbf{H}_h$ and $\mathbf{Q}_{\tilde{h}}$. We consider the Raviart-Thomas space of lowest order

$$H_h^{\boldsymbol{\sigma}} := \left\{ \boldsymbol{\tau}_h \in H(\mathbf{div};\Omega) \,:\, \boldsymbol{\tau}_h|_T \in [\mathcal{RT}_0(T)^{\mathtt{t}}]^2, \quad \forall T \in \mathcal{T}_h \right\}, \tag{2.8}$$

and the finite element spaces

$$H_{D,h}^{\mathbf{u}} := \left\{ \mathbf{v}_h \in [C(\bar{\Omega}) \cap H^1_{\Gamma_D}(\Omega)]^2 \,:\, \mathbf{v}_h|_T \in [\mathcal{P}_1(T)]^2, \quad \forall T \in \mathcal{T}_h \right\}, \tag{2.9}$$

$$H_h^{\boldsymbol{\gamma}} := \left\{ \boldsymbol{\eta}_h \in [L^2(\Omega)]^{2\times 2}_{\mathtt{skew}} \,:\, \boldsymbol{\eta}_h|_T \in [\mathcal{P}_0(T)]^{2\times 2}, \quad \forall T \in \mathcal{T}_h \right\}. \tag{2.10}$$

Then, we define $\mathbf{H}_h := H_h^{\boldsymbol{\sigma}} \times H_{D,h}^{\mathbf{u}} \times H_h^{\boldsymbol{\gamma}}$. On the other hand, let $\gamma_{\tilde{h}} = \{\tilde{e}_1, \tilde{e}_2, ..., \tilde{e}_m\}$ be an independent partition of the Neumann boundary Γ_N with $\tilde{h} := \max\{|\tilde{e}_j| : j = 1, ..., m\}$. We define the finite element subspace

$$\mathbf{Q}_{\tilde{h}} := \left\{ \boldsymbol{\chi}_{\tilde{h}} \in [C(\Gamma_N) \cap H^{1/2}_{00}(\Gamma_N)]^2 \,:\, \boldsymbol{\chi}_{\tilde{h}}|_{\tilde{e}_j} \in [\mathcal{P}_1(\tilde{e}_j)]^2, \quad \forall j \in \{1, ..., m\} \right\}. \tag{2.11}$$

Then, the discrete null space of the bilinear form B reduces to $\mathbf{V}_{h,\tilde{h}} = V_{h,\tilde{h}} \times H_{D,h}^{\mathbf{u}} \times H_h^{\boldsymbol{\gamma}}$, where

$$V_{h,\tilde{h}} := \left\{ \boldsymbol{\tau}_h \in H_h^{\boldsymbol{\sigma}} :\ \langle \boldsymbol{\tau}_h \mathbf{n}, \boldsymbol{\chi}_{\tilde{h}} \rangle_{\Gamma_N} = 0 \quad \forall \boldsymbol{\chi}_{\tilde{h}} \in \mathbf{Q}_{\tilde{h}} \right\}.$$

We remark that, in general, $V_{h,\tilde{h}}$ is not included in $\mathbf{V}$.

Let $\{e_1, e_2, ..., e_n\}$ be the partition of Γ_N inherited from the triangulation $\mathcal{T}_h$. We assume that the family of triangulations $\{\mathcal{T}_h\}_{h>0}$ is uniformly regular near Γ_N, which means that there exists $C > 0$, independent of h, such that $|e_j| \geq C\,h$, $\forall\, j \in \{1, ..., n\}$ and $\forall\, h > 0$. We also assume that the independent partitions $\{\gamma_{\tilde{h}}\}_{\tilde{h}>0}$ of Γ_N are uniformly regular, that is, there exists $C > 0$, independent of $\tilde{h}$, such that $|\tilde{e}_j| \geq C\,\tilde{h}$, $\forall\, j \in \{1, ..., m\}$, $\forall\, \tilde{h} > 0$. These assumptions on $\{\mathcal{T}_h\}_{h>0}$ and $\{\gamma_{\tilde{h}}\}_{\tilde{h}>0}$ are used in [17] to prove that the bilinear form $B(\cdot,\cdot)$ satisfies the discrete inf-sup condition (see Lemmas 4.6 and 4.7 in [17]). Then, the augmented Galerkin scheme (2.7) is shown to be well-posed and a Cea estimate is obtained $\forall\,\tilde{h}\;\le\;h_0$ and $\forall\,h\;\le\;C_0\,\tilde{h}$; cf. Theorem 4.9 in [17]. Let us remark here that the asymptotic assumption $\tilde{h}\;\le\;h_0$ can be removed; cf. [19]. Indeed, instead of the approximation property $(\mathrm{AP}^{\boldsymbol{\xi}}_{\tilde{h}})$ assumed in [17, section 4.2], one should assume that there exists a fixed $\boldsymbol{\chi}\in[H^{1/2}_{00}(\Gamma_N)]^2$ such that

$$\boldsymbol{\chi}\in\mathbf{Q}_{\tilde{h}}\quad\forall\,\tilde{h}>0\quad\text{and}\;\langle\mathbf{n},\boldsymbol{\chi}\rangle_{\Gamma_N}\neq 0. \tag{2.12}$$

Such a function $\boldsymbol{\chi}$ can be constructed following the ideas of [21]. Then, instead of applying [17, Lemma 4.4] to prove the coerciveness of the bilinear form $A(\cdot,\cdot)$ on the discrete kernel, one should apply the following result.

Lemma 2.1 *There exists $C>0$, independent of h and $\tilde{h}$, such that*

$$||\boldsymbol{\tau}_h||^2_{H(\mathbf{div};\,\Omega)}\;\le\;C\,||\boldsymbol{\tau}_{0h}||^2_{H(\mathbf{div};\,\Omega)}\quad\forall\,\boldsymbol{\tau}_h\in V_{h,\tilde{h}}\,.$$

Proof. Let $\boldsymbol{\tau}_h\in V_{h,\tilde{h}}$. Then, we can write $\boldsymbol{\tau}_h=\boldsymbol{\tau}_{0h}+d_h\,\mathbf{I}$, with $\boldsymbol{\tau}_{0h}\in H^{\boldsymbol{\sigma}}_h$, $\int_\Omega \mathrm{tr}(\boldsymbol{\tau}_{0h})=0$, and $d_h\in\mathbb{R}$. It follows that

$$0=\langle\boldsymbol{\tau}_h\mathbf{n},\boldsymbol{\chi}\rangle_{\Gamma_N}=\langle\boldsymbol{\tau}_{0h}\mathbf{n},\boldsymbol{\chi}\rangle_{\Gamma_N}+d_h\langle\mathbf{n},\boldsymbol{\chi}\rangle_{\Gamma_N}\quad\forall\,\boldsymbol{\chi}\in[H^{1/2}_{00}(\Gamma_N)]^2,$$

and for $\boldsymbol{\chi}$ satisfying (2.12), we obtain

$$d_h\;=\;-\frac{\langle\boldsymbol{\tau}_{0h}\mathbf{n},\boldsymbol{\chi}\rangle_{\Gamma_N}}{\langle\mathbf{n},\boldsymbol{\chi}\rangle_{\Gamma_N}}$$

Applying a trace theorem,

$$|d_h|\;\le\;C\,\frac{||\boldsymbol{\chi}||_{[H^{1/2}_{00}(\Gamma_N)]^2}}{|\langle\mathbf{n},\boldsymbol{\chi}\rangle_{\Gamma_N}|}\,||\boldsymbol{\tau}_{0h}||_{H(\mathbf{div};\,\Omega)}.$$

Then, the result follows noting that $||\boldsymbol{\tau}_h||^2_{H(\mathbf{div};\,\Omega)}=||\boldsymbol{\tau}_{0h}||^2_{H(\mathbf{div};\,\Omega)}+2\,d_h^2\,|\Omega|$. □

The rate of convergence of the Galerkin scheme (2.7) when the finite element subspaces $H^{\boldsymbol{\sigma}}_h$, $H^{\mathbf{u}}_{D,h}$, $H^{\boldsymbol{\gamma}}_h$ and $\mathbf{Q}_{\tilde{h}}$ defined in (2.8)-(2.11) are used is stated in Theorem 4.10 in [17]. Due the previous remarks, the asymptotic assumption $\tilde{h}\;\le\;h_0$ can also be removed from that theorem.

2.3 Residual-based a posteriori error analysis

In this section we derive an a posteriori error estimator of residual type for the discrete scheme (2.7). In what follows, we assume that $h\le C_0\,\tilde{h}$. Then, we can assume, without loss of generality, that each side $e_i\in E_h(\Gamma_N)$, $i\in\{1,\dots,n\}$, is contained in a side $\tilde{e}_j$, for some $j\in\{1,\dots,m\}$; in this case, we denote by $\tilde{h}_{e_i}=|\tilde{e}_j|$. Further, given $\boldsymbol{\tau}\in[L^2(\Omega)]^{2\times 2}$ such that $\boldsymbol{\tau}|_T\in[C(T)]^{2\times 2}$ on each $T\in\mathcal{T}_h$, an edge $e\in E(T)\cap E_h(\Omega)$, for some $T\in\mathcal{T}_h$, and the unit tangential vector $\mathbf{t}_T$ along e, we denote by $J[\boldsymbol{\tau}\mathbf{t}_T]$ the jump of $\boldsymbol{\tau}$ across e, that is, $J[\boldsymbol{\tau}\mathbf{t}_T] := (\boldsymbol{\tau}|_T - \boldsymbol{\tau}|_{T'})|_e \mathbf{t}_T$, where $T' \in \mathcal{T}_h$ is such that $T \cap T' = e$. Abusing notation, when $e \in E_h(\Gamma)$, we write $J[\boldsymbol{\tau}\mathbf{t}_T] := \boldsymbol{\tau}|_e \mathbf{t}_T$. We recall here that, if $\mathbf{n}_T := (n_1, n_2)^{\mathtt{t}}$ is the unit outward normal to ∂T, then $\mathbf{t}_T := (-n_2, n_1)^{\mathtt{t}}$. The normal jumps $J[\boldsymbol{\tau}\mathbf{n}_T]$ can be defined analogously. Finally, from now on we assume that piecewise constant tensors are contained in $H_h^{\boldsymbol{\sigma}}$.

Now, for any $T \in \mathcal{T}_h$, we consider the local error indicator θ_T, defined as follows:

$$
\begin{aligned}
\theta_T^2 \;:=\; & \|\mathbf{f} + \mathbf{div}(\boldsymbol{\sigma}_h)\|^2_{[L^2(T)]^2} \;+\; \tfrac{1}{4}\,\|\boldsymbol{\sigma}_h - \boldsymbol{\sigma}_h^{\mathtt{t}}\|^2_{[L^2(T)]^{2\times 2}} \;+\; \|\boldsymbol{\gamma}_h - \tfrac{1}{2}(\nabla \mathbf{u}_h - (\nabla \mathbf{u}_h)^{\mathtt{t}})\|^2_{[L^2(T)]^{2\times 2}} \\
& + h_T^2 \left(\|\,\mathbf{curl}(\mathcal{C}^{-1}\boldsymbol{\sigma}_h - \nabla \mathbf{u}_h + \boldsymbol{\gamma}_h)\|^2_{[L^2(T)]^2} \;+\; \|\,\mathbf{curl}(\mathcal{C}^{-1}(\boldsymbol{\varepsilon}(\mathbf{u}_h) - \mathcal{C}^{-1}\boldsymbol{\sigma}_h))\|^2_{[L^2(T)]^2} \right) \\
& + \sum_{e \in E(T)} h_e \left(\|J[(\mathcal{C}^{-1}\boldsymbol{\sigma}_h - \nabla \mathbf{u}_h + \boldsymbol{\gamma}_h)\mathbf{t}_T]\|^2_{[L^2(e)]^2} \;+\; \|J[(\mathcal{C}^{-1}(\boldsymbol{\varepsilon}(\mathbf{u}_h) - \mathcal{C}^{-1}\boldsymbol{\sigma}_h))\mathbf{t}_T]\|^2_{[L^2(e)]^2} \right) \\
& + h_T^2 \left(\|\mathbf{div}(\boldsymbol{\varepsilon}(\mathbf{u}_h) - \frac{1}{2}\,\mathcal{C}^{-1}(\boldsymbol{\sigma}_h + \boldsymbol{\sigma}_h^{\mathtt{t}}))\|^2_{[L^2(T)]^2} + \|\mathbf{div}(\boldsymbol{\gamma}_h - \frac{1}{2}(\nabla \mathbf{u}_h - (\nabla \mathbf{u}_h)^{\mathtt{t}}))\|^2_{[L^2(T)]^2} \right) \\
& + \sum_{e \in E(T) \cap E_h(\Omega \cup \Gamma_N)} h_e\, \|J[(\boldsymbol{\varepsilon}(\mathbf{u}_h) - \frac{1}{2}\,\mathcal{C}^{-1}(\boldsymbol{\sigma}_h + \boldsymbol{\sigma}_h^{\mathtt{t}}))\mathbf{n}_T]\|^2_{[L^2(e)]^2} \\
& + \sum_{e \in E(T) \cap E_h(\Omega \cup \Gamma_N)} h_e\, \|J[(\boldsymbol{\gamma}_h - \frac{1}{2}(\nabla \mathbf{u}_h - (\nabla \mathbf{u}_h)^{\mathtt{t}}))\mathbf{n}_T]\|^2_{[L^2(e)]^2} \\
& + \sum_{e \in E(T) \cap E_h(\Gamma_N)} h_e \Big(\log(1+\kappa)\, \|\mathbf{g} - \boldsymbol{\sigma}_h \mathbf{n}_T\|^2_{[L^2(e)]^2} + \left\| \frac{\partial}{\partial\, \mathbf{t}_T}(\mathbf{u}_h + \boldsymbol{\xi}_{\tilde{h}}) \right\|^2_{[L^2(e)]^2} \Big)
\end{aligned}
\tag{2.13}
$$

where $\kappa = \max\{\frac{\tilde{h}_j}{\tilde{h}_k} : \tilde{e}_j \text{ and } \tilde{e}_k \text{ neighbours}\}$. We remark that if we set $\Gamma_N = \emptyset$ we recover the a posteriori error estimator obtained in [8]. The residual character of each term on the right hand side of (2.13) is clear. We state below the main result of this section, that is, that the global residual error estimator $\theta := \left(\sum_{T \in \mathcal{T}_h} \theta_T^2 \right)^{1/2}$ is both reliable and efficient.

Theorem 2.2 *Let $((\boldsymbol{\sigma}, \mathbf{u}, \boldsymbol{\gamma}), \boldsymbol{\xi}) \in \mathbf{H} \times \mathbf{Q}$ and $((\boldsymbol{\sigma}_h, \mathbf{u}_h, \boldsymbol{\gamma}_h), \boldsymbol{\xi}_{\tilde{h}}) \in \mathbf{H}_h \times \mathbf{Q}_{\tilde{h}}$ be the unique solution to problems* (2.3) *and* (2.7)*, respectively, and let us assume that $\mathbf{g} \in [L^2(\Gamma_N)]^2$. Then, there exist positive constants, $C_{\mathtt{eff}}$ and $C_{\mathtt{rel}}$, independent of λ, h and $\tilde{h}$, such that*

$$
C_{\mathtt{eff}}\, \theta \;\le\; \|((\boldsymbol{\sigma} - \boldsymbol{\sigma}_h, \mathbf{u} - \mathbf{u}_h, \boldsymbol{\gamma} - \boldsymbol{\gamma}_h), \boldsymbol{\xi} - \boldsymbol{\xi}_{\tilde{h}})\|_{\mathbf{H} \times \mathbf{Q}} \;\le\; C_{\mathtt{rel}}\, \theta\,. \tag{2.14}
$$

The reliability (upper bound in (2.14)) is proved in subsection 2.3.1 below; the so-called efficiency (lower bound in (2.14)) is proved in subsection 2.3.2.

2.3.1 Reliability

The proof of reliability is similar to that of [8]. We let $(\mathbf{z}, \boldsymbol{\sigma}^*) \in [H^1_{\Gamma_D}(\Omega)]^2 \times H(\mathbf{div};\Omega)$ be the unique solution to the boundary value problem

$$\left\{ \begin{array}{rcll} \boldsymbol{\sigma}^* &=& \boldsymbol{\varepsilon}(\mathbf{z}) & \text{in } \Omega \\ -\mathbf{div}(\boldsymbol{\sigma}^*) &=& \mathbf{f} + \mathbf{div}(\boldsymbol{\sigma}_h) & \text{in } \Omega \\ \mathbf{z} &=& \mathbf{0} & \text{on } \Gamma_D \\ \boldsymbol{\sigma}^*\mathbf{n} &=& \mathbf{g} - \boldsymbol{\sigma}_h\mathbf{n} & \text{on } \Gamma_N \,. \end{array} \right.$$

Then, we use the continuous dependence of the solution on the data to obtain that

$$||\boldsymbol{\sigma}^*||_{H(\mathbf{div};\Omega)} \leq C \Big(||\mathbf{f} + \mathbf{div}(\boldsymbol{\sigma}_h)||_{[L^2(\Omega)]^2} + ||\mathbf{g} - \boldsymbol{\sigma}_h\mathbf{n}||_{[H^{-1/2}(\Gamma_N)]^2} \Big), \tag{2.15}$$

where the $[H^{-1/2}(\Gamma_N)]^2$-norm can be bounded in terms of a L^2-norm, assuming that $\mathbf{g} \in [L^2(\Gamma_N)]^2$ and applying Theorem 2 in [10], as follows:

$$\begin{aligned} ||\mathbf{g} - \boldsymbol{\sigma}_h\mathbf{n}||^2_{[H^{-1/2}(\Gamma_N)]^2} &\leq C \log(1+\kappa) \sum_{j=1}^{m} |\tilde{e}_j| \, ||\mathbf{g} - \boldsymbol{\sigma}_h\mathbf{n}||^2_{[L^2(\tilde{e}_j)]^2} \\ &= C \log(1+\kappa) \sum_{e \in E_h(\Gamma_N)} \tilde{h}_e \, ||\mathbf{g} - \boldsymbol{\sigma}_h\mathbf{n}||^2_{[L^2(e)]^2} \,. \end{aligned} \tag{2.16}$$

On the other hand, we remark that $(\boldsymbol{\sigma} - \boldsymbol{\sigma}_h - \boldsymbol{\sigma}^*)\mathbf{n} = \mathbf{0}$ on Γ_N and use that $A(\cdot,\cdot)$ is coercive in $\mathbf{V}$ and linear in the first argument to deduce that

$$\begin{aligned} &\alpha \, ||(\boldsymbol{\sigma} - \boldsymbol{\sigma}_h - \boldsymbol{\sigma}^*, \mathbf{u} - \mathbf{u}_h, \boldsymbol{\gamma} - \boldsymbol{\gamma}_h)||^2_{\mathbf{H}} \leq \\ &\qquad \leq A((\boldsymbol{\sigma} - \boldsymbol{\sigma}_h, \mathbf{u} - \mathbf{u}_h, \boldsymbol{\gamma} - \boldsymbol{\gamma}_h), (\boldsymbol{\sigma} - \boldsymbol{\sigma}_h - \boldsymbol{\sigma}^*, \mathbf{u} - \mathbf{u}_h, \boldsymbol{\gamma} - \boldsymbol{\gamma}_h)) \\ &\qquad - A((\boldsymbol{\sigma}^*, \mathbf{0}, \mathbf{0}), (\boldsymbol{\sigma} - \boldsymbol{\sigma}_h - \boldsymbol{\sigma}^*, \mathbf{u} - \mathbf{u}_h, \boldsymbol{\gamma} - \boldsymbol{\gamma}_h)) \,. \end{aligned}$$

Now, we remark that $\mathbf{div}(\boldsymbol{\sigma} - \boldsymbol{\sigma}_h - \boldsymbol{\sigma}^*) = \mathbf{0}$ in Ω and use that A is bounded in $\mathbf{H}$ to obtain

$$\begin{aligned} &\alpha \, ||(\boldsymbol{\sigma} - \boldsymbol{\sigma}_h - \boldsymbol{\sigma}^*, \mathbf{u} - \mathbf{u}_h, \boldsymbol{\gamma} - \boldsymbol{\gamma}_h)||_{\mathbf{H}} \leq \\ &\qquad \leq \sup_{\substack{(\boldsymbol{\tau},\mathbf{v},\boldsymbol{\eta}) \in \mathbf{V} \\ \mathbf{div}(\boldsymbol{\tau}) = \mathbf{0} \\ (\boldsymbol{\tau},\mathbf{v},\boldsymbol{\eta}) \neq \mathbf{0}}} \frac{|A((\boldsymbol{\sigma} - \boldsymbol{\sigma}_h, \mathbf{u} - \mathbf{u}_h, \boldsymbol{\gamma} - \boldsymbol{\gamma}_h), (\boldsymbol{\tau}, \mathbf{v}, \boldsymbol{\eta}))|}{||(\boldsymbol{\tau}, \mathbf{v}, \boldsymbol{\eta})||_{\mathbf{H}}} + M \, ||\boldsymbol{\sigma}^*||_{H(\mathbf{div};\Omega)}. \end{aligned} \tag{2.17}$$

It only remains to bound the first term on the right hand side of (2.17). Let $(\boldsymbol{\tau}, \mathbf{v}, \boldsymbol{\eta}) \in \mathbf{V} \setminus \{\mathbf{0}\}$ such that $\mathbf{div}(\boldsymbol{\tau}) = \mathbf{0}$ in Ω. Since Ω is simply connected, there exists a stream function $\boldsymbol{\varphi} \in [H^1(\Omega)]^2$ such that $\int_\Omega \varphi_i = 0$ $(i = 1, 2)$ and $\boldsymbol{\tau} = \underline{\mathbf{curl}}(\boldsymbol{\varphi})$. We remark that

$$||\boldsymbol{\varphi}||_{[H^1(\Omega)]^2} \leq C \, |\boldsymbol{\varphi}|_{[H^1(\Omega)]^2} \leq C \, ||\boldsymbol{\tau}||_{H(\mathbf{div};\Omega)} \,. \tag{2.18}$$

Then, we define

$$\boldsymbol{\varphi}_h := (\varphi_{1,h}, \varphi_{2,h}), \quad \varphi_{i,h} := I_h(\varphi_i) \quad (i = 1,2), \qquad \boldsymbol{\tau}_h := \underline{\mathbf{curl}}(\boldsymbol{\varphi}_h) \tag{2.19}$$

and remark that $\boldsymbol{\tau}_h \in H_h^{\boldsymbol{\sigma}}$ and $\mathbf{div}(\boldsymbol{\tau}_h) = \mathbf{0}$ in Ω. Then, we decompose

$$\begin{aligned} A((\boldsymbol{\sigma} - \boldsymbol{\sigma}_h, \mathbf{u} - \mathbf{u}_h, \boldsymbol{\gamma} - \boldsymbol{\gamma}_h), (\boldsymbol{\tau}, \mathbf{v}, \boldsymbol{\eta})) \;&=\; A((\boldsymbol{\sigma} - \boldsymbol{\sigma}_h, \mathbf{u} - \mathbf{u}_h, \boldsymbol{\gamma} - \boldsymbol{\gamma}_h), (\boldsymbol{\tau}_h, \mathbf{v}_h, \mathbf{0})) \\ &\quad + A((\boldsymbol{\sigma} - \boldsymbol{\sigma}_h, \mathbf{u} - \mathbf{u}_h, \boldsymbol{\gamma} - \boldsymbol{\gamma}_h), (\boldsymbol{\tau} - \boldsymbol{\tau}_h, \mathbf{v} - \mathbf{v}_h, \boldsymbol{\eta})) \end{aligned}$$

and use that $(\boldsymbol{\sigma}, \mathbf{u}, \boldsymbol{\gamma})$ and $(\boldsymbol{\sigma}_h, \mathbf{u}_h, \boldsymbol{\gamma}_h)$ are the solutions to problems (2.3) and (2.7), respectively, the definitions of the forms F and B, that $\mathbf{div}(\boldsymbol{\tau}) = \mathbf{div}(\boldsymbol{\tau}_h) = \mathbf{0}$ in Ω and $\boldsymbol{\tau}\mathbf{n} = \mathbf{0}$ on Γ_N, to get

$$\begin{aligned} &A((\boldsymbol{\sigma} - \boldsymbol{\sigma}_h, \mathbf{u} - \mathbf{u}_h, \boldsymbol{\gamma} - \boldsymbol{\gamma}_h), (\boldsymbol{\tau}, \mathbf{v}, \boldsymbol{\eta})) \\ &\quad = \int_\Omega \mathbf{f} \cdot (\mathbf{v} - \mathbf{v}_h) - \langle (\boldsymbol{\tau} - \boldsymbol{\tau}_h)\mathbf{n}, \boldsymbol{\xi}_{\tilde{h}} \rangle_{\Gamma_N} - A((\boldsymbol{\sigma}_h, \mathbf{u}_h, \boldsymbol{\gamma}_h), (\boldsymbol{\tau} - \boldsymbol{\tau}_h, \mathbf{v} - \mathbf{v}_h, \boldsymbol{\eta})). \end{aligned}$$

Integrating by parts and making some algebraic manipulations, we obtain that

$$\begin{aligned} &A((\boldsymbol{\sigma} - \boldsymbol{\sigma}_h, \mathbf{u} - \mathbf{u}_h, \boldsymbol{\gamma} - \boldsymbol{\gamma}_h), (\boldsymbol{\tau}, \mathbf{v}, \boldsymbol{\eta})) \;= \\ &\quad = \int_\Omega (\mathbf{f} + \mathbf{div}(\boldsymbol{\sigma}_h)) \cdot (\mathbf{v} - \mathbf{v}_h) - \langle (\boldsymbol{\tau} - \boldsymbol{\tau}_h)\mathbf{n}, \mathbf{u}_h + \boldsymbol{\xi}_{\tilde{h}} \rangle_{\Gamma_N} \\ &\quad - \int_\Omega (\boldsymbol{\tau} - \boldsymbol{\tau}_h) : \Big(\big(\mathcal{C}^{-1}\boldsymbol{\sigma}_h - \nabla \mathbf{u}_h + \boldsymbol{\gamma}_h \big) - \kappa_1 \, \mathcal{C}^{-1} \big(\boldsymbol{\varepsilon}(\mathbf{u}_h) - \mathcal{C}^{-1}\boldsymbol{\sigma}_h \big) \Big) \\ &\quad - \int_\Omega \nabla (\mathbf{v} - \mathbf{v}_h) : \Big(\kappa_1 \Big(\boldsymbol{\varepsilon}(\mathbf{u}_h) - \mathcal{C}^{-1} \big(\frac{\boldsymbol{\sigma}_h + \boldsymbol{\sigma}_h^{\mathtt{t}}}{2} \big) \Big) + \kappa_3 \Big(\boldsymbol{\gamma}_h - \frac{\nabla \mathbf{u}_h - (\nabla \mathbf{u}_h)^{\mathtt{t}}}{2} \Big) \Big) \\ &\quad + \int_\Omega \boldsymbol{\eta} : \Big(\frac{\boldsymbol{\sigma}_h - \boldsymbol{\sigma}_h^{\mathtt{t}}}{2} - \kappa_3 \big(\boldsymbol{\gamma}_h - \frac{\nabla \mathbf{u}_h - (\nabla \mathbf{u}_h)^{\mathtt{t}}}{2} \big) \Big). \end{aligned} \tag{2.20}$$

All the terms appearing on the right hand side of (2.20), except the second one, yet appeared in [8] and can be bounded using the same techniques. More specifically, the first and the last terms are bounded using the Cauchy-Schwarz inequality. Concerning terms involving $\boldsymbol{\tau} - \boldsymbol{\tau}_h$, we write them in terms of the stream functions, $\boldsymbol{\varphi}$ and $\boldsymbol{\varphi}_h$, integrate by parts and use the error estimates for the Clément interpolation operator (see Lemma 1.1). In particular, the second term on the right hand side of (2.20) can be written as follows (see also [7]):

$$\langle (\boldsymbol{\tau} - \boldsymbol{\tau}_h)\mathbf{n}, \mathbf{u}_h + \boldsymbol{\xi}_{\tilde{h}} \rangle_{\Gamma_N} = \sum_{T \in \mathcal{T}_h} \sum_{e \in E(T) \cap E_h(\Gamma_N)} \int_e (\boldsymbol{\varphi} - \boldsymbol{\varphi}_h) \frac{\partial}{\partial \mathbf{t}} (\mathbf{u}_h + \boldsymbol{\xi}_{\tilde{h}}),$$

where we used that $-\underline{\mathbf{curl}}(\mathbf{w}) \cdot \mathbf{n}$ is the tangential derivative of $\mathbf{w}$, $\frac{\partial \mathbf{w}}{\partial \mathbf{t}}$. Then, we use the Cauchy-Schwarz inequality, Lemma 1.1, that the number of triangles in $\Delta(e)$ is bounded and (2.18) to obtain that

$$|\langle(\boldsymbol{\tau}-\boldsymbol{\tau}_h)\mathbf{n}, \mathbf{u}_h+\boldsymbol{\xi}_{\tilde{h}}\rangle_{\Gamma_N}| \leq C\,\Big(\sum_{T\in\mathcal{T}_h}\ \sum_{e\in E(T)\cap E_h(\Gamma_N)} h_e\left|\left|\frac{\partial}{\partial\,\mathbf{t}}(\mathbf{u}_h+\boldsymbol{\xi}_{\tilde{h}})\right|\right|^2_{[L^2(e)]^2}\Big)^{1/2}||\boldsymbol{\tau}||_{H(\mathbf{div};\,\Omega)}.$$

Finally, in order to bound the term involving $\nabla(\mathbf{v}-\mathbf{v}_h)$, we choose $\mathbf{v}_h = (I_h v_1, I_h v_2)$, integrate by parts and use Lemma 1.1. We observe that, since now $\mathbf{v}$ and $\mathbf{v}_h$ vanish only on Γ_D, integration by parts causes the appearance of normal jumps on the Neumann boundary Γ_N. Then, using the triangular inequality, (2.15), (2.16), (2.17), (2.20) and the previous considerations, we deduce that

$$||(\boldsymbol{\sigma}-\boldsymbol{\sigma}_h, \mathbf{u}-\mathbf{u}_h, \boldsymbol{\gamma}-\boldsymbol{\gamma}_h)||_{\mathbf{H}} \leq C\,\theta \tag{2.21}$$

with C independent of λ, h and $\tilde{h}$.

It remains to bound $||\boldsymbol{\xi}-\boldsymbol{\xi}_{\tilde{h}}||_{\mathbf{Q}}$. With that purpose, we extend the proof of Theorem 4.3 in [7]. Since $\boldsymbol{\xi}-\boldsymbol{\xi}_{\tilde{h}} \in \mathbf{Q}$, we can use (2.6) to obtain

$$||\boldsymbol{\xi}-\boldsymbol{\xi}_{\tilde{h}}||_{\mathbf{Q}} \leq \frac{1}{\beta}\sup_{\substack{\boldsymbol{\tau}\in H_0\\ \boldsymbol{\tau}\neq\mathbf{0}}}\frac{\langle\boldsymbol{\tau}\mathbf{n}, \boldsymbol{\xi}-\boldsymbol{\xi}_{\tilde{h}}\rangle_{\Gamma_N}}{||\boldsymbol{\tau}||_{H(\mathbf{div};\,\Omega)}}\,.$$

Let $\boldsymbol{\tau}\in H_0\setminus\{\mathbf{0}\}$ and let $\boldsymbol{\varphi}\in[H^1(\Omega)]^2$ such that $\int_\Omega \boldsymbol{\varphi}_i = 0$ $(i=1,2)$ and $\boldsymbol{\tau} = \underline{\mathbf{curl}}(\boldsymbol{\varphi})$. We consider $\boldsymbol{\varphi}_h$ and $\boldsymbol{\tau}_h$ defined as in (2.19), and take $(\mathbf{v},\boldsymbol{\eta}) = (\mathbf{0},\mathbf{0})$ in (2.3) and $(\mathbf{v}_h,\boldsymbol{\eta}_h) = (\mathbf{0},\mathbf{0})$ in (2.7) to obtain

$$\begin{aligned}\langle\boldsymbol{\tau}\mathbf{n}, \boldsymbol{\xi}-\boldsymbol{\xi}_{\tilde{h}}\rangle_{\Gamma_N} \;=\; &-A((\boldsymbol{\sigma}-\boldsymbol{\sigma}_h, \mathbf{u}-\mathbf{u}_h, \boldsymbol{\gamma}-\boldsymbol{\gamma}_h), (\boldsymbol{\tau},\mathbf{0},\mathbf{0})) \;-\; \langle(\boldsymbol{\tau}-\boldsymbol{\tau}_h)\mathbf{n}, \boldsymbol{\xi}_{\tilde{h}}\rangle_{\Gamma_N}\\ &- A((\boldsymbol{\sigma}_h, \mathbf{u}_h, \boldsymbol{\gamma}_h), (\boldsymbol{\tau}-\boldsymbol{\tau}_h, \mathbf{0},\mathbf{0})).\end{aligned}$$

Integrating by parts and using that $\mathbf{div}(\boldsymbol{\tau}) = \mathbf{div}(\boldsymbol{\tau}_h) = \mathbf{0}$ in Ω, we have that

$$\begin{aligned}\langle\boldsymbol{\tau}\mathbf{n}, \boldsymbol{\xi}-\boldsymbol{\xi}_{\tilde{h}}\rangle_{\Gamma_N} = &-A((\boldsymbol{\sigma}-\boldsymbol{\sigma}_h, \mathbf{u}-\mathbf{u}_h, \boldsymbol{\gamma}-\boldsymbol{\gamma}_h), (\boldsymbol{\tau},\mathbf{0},\mathbf{0})) - \langle(\boldsymbol{\tau}-\boldsymbol{\tau}_h)\mathbf{n}, \mathbf{u}_h+\boldsymbol{\xi}_{\tilde{h}}\rangle_{\Gamma_N}\\ &- \int_\Omega(\boldsymbol{\tau}-\boldsymbol{\tau}_h) : \Big(\big(\mathcal{C}^{-1}\boldsymbol{\sigma}_h - \nabla\mathbf{u}_h + \boldsymbol{\gamma}_h\big) - \kappa_1\,\mathcal{C}^{-1}\big(\boldsymbol{\varepsilon}(\mathbf{u}_h) - \mathcal{C}^{-1}\boldsymbol{\sigma}_h\big)\Big).\end{aligned}$$

Finally, using that A is bounded and proceeding with the remaining terms as before, we deduce that

$$||\boldsymbol{\xi}-\boldsymbol{\xi}_{\tilde{h}}||_{\mathbf{Q}} \leq \frac{M}{\beta}||(\boldsymbol{\sigma}-\boldsymbol{\sigma}_h, \mathbf{u}-\mathbf{u}_h, \boldsymbol{\gamma}-\boldsymbol{\gamma}_h)||_{\mathbf{H}} + C\,\theta\,. \tag{2.22}$$

Inequalities (2.21) and (2.22) imply the reliability of the a posteriori error estimator θ.

2.3.2 Efficiency

The a posteriori error estimator θ_T defined in (2.13) and the one given in [8] differ only in the last two terms and in the terms involving normal jumps across the edges of Γ_N. The remaining terms can be bounded from above using Lemmas 4.7-4.10 in [8].

In order to bound the term involving the tangential derivative of $\mathbf{u}_h + \boldsymbol{\xi}_{\tilde{h}}$, we follow the proof of Lemma 4.5 in [7]. Given $e \in E_h(\Gamma_N)$, we denote $\mathbf{v}_e := \frac{\partial}{\partial \mathbf{t}_T}(\mathbf{u}_h + \boldsymbol{\xi}_{\tilde{h}})$ on e. Then, using that $\mathbf{u} = -\boldsymbol{\xi}$ on Γ_N, we can write $\mathbf{v}_e = \frac{\partial}{\partial \mathbf{t}_T}(\mathbf{u}_h - \mathbf{u}) + \frac{\partial}{\partial \mathbf{t}_T}(\boldsymbol{\xi}_{\tilde{h}} - \boldsymbol{\xi})$ on e, and assuming that $\mathbf{v}_e \in [\mathcal{P}_k(e)]^2$, we have that

$$\sum_{e \in E_h(\Gamma_N)} h_e \, ||\mathbf{v}_e||^2_{[L^2(e)]^2} \le C \Big(\int_\Gamma \hat{\boldsymbol{\psi}} \cdot \frac{\partial}{\partial \mathbf{t}_T}(\mathbf{u}_h - \mathbf{u}) + \int_\Gamma \hat{\boldsymbol{\psi}} \cdot \frac{\partial \hat{\boldsymbol{\xi}}}{\partial \mathbf{t}_T} \Big)$$

where we denote

$$\hat{\boldsymbol{\psi}} := \begin{cases} \boldsymbol{\psi} & \text{on } \Gamma_N \\ \mathbf{0} & \text{on } \Gamma_D \end{cases} \qquad \hat{\boldsymbol{\xi}} := \begin{cases} \boldsymbol{\xi}_{\tilde{h}} - \boldsymbol{\xi} & \text{on } \Gamma_N \\ \mathbf{0} & \text{on } \Gamma_D \end{cases}$$

with $\boldsymbol{\psi} := \psi_e h_e \mathbf{v}_e$ on each edge $e \in E_h(\Gamma_N)$. Since $\boldsymbol{\psi}$, $\boldsymbol{\xi}_{\tilde{h}} - \boldsymbol{\xi} \in [H^{1/2}_{00}(\Gamma_N)]^2$, then $\hat{\boldsymbol{\psi}}$, $\hat{\boldsymbol{\xi}} \in [H^{1/2}(\Gamma)]^2$, and the norms $||\cdot||_{[H^{1/2}_{00}(\Gamma_N)]^2}$ and $||\cdot||_{[H^{1/2}(\Gamma)]^2}$ of the corresponding functions and their extensions are equivalent. Then, we apply the Cauchy-Schwarz inequality, Lemma 1.3, that the tangential operator is bounded and a trace theorem, and deduce that

$$\begin{aligned} \sum_{e \in E_h(\Gamma_N)} h_e ||\mathbf{v}_e||^2_{[L^2(e)]^2} &\le C \left|\left|\hat{\boldsymbol{\psi}}\right|\right|_{[H^{1/2}(\Gamma)]^2} \left(\left|\left| \frac{\partial\,(\mathbf{u}_h - \mathbf{u})}{\partial \mathbf{t}_T} \right|\right|_{[H^{-1/2}(\Gamma)]^2} + \left|\left| \frac{\partial \hat{\boldsymbol{\xi}}}{\partial \mathbf{t}_T} \right|\right|_{[H^{-1/2}(\Gamma)]^2} \right) \\ &\le C\, h^{-1/2} \left|\left|\hat{\boldsymbol{\psi}}\right|\right|_{[L^2(\Gamma)]^2} \Big(||\mathbf{u}_h - \mathbf{u}||_{[H^1(\Omega)]^2} + ||\boldsymbol{\xi}_{\tilde{h}} - \boldsymbol{\xi}||_{[H^{1/2}_{00}(\Gamma_N)]^2} \Big). \end{aligned}$$

Then, since $0 \le \psi_e \le 1$, we have that

$$\left|\left|\hat{\boldsymbol{\psi}}\right|\right|^2_{[L^2(\Gamma)]^2} = \int_{\Gamma_N} \psi_e^2 h_e^2 |\mathbf{v}_e|^2 \le h \sum_{e \in E_h(\Gamma_N)} h_e ||\mathbf{v}_e||^2_{[L^2(e)]^2}$$

and, therefore

$$\sum_{e \in E_h(\Gamma_N)} h_e ||\mathbf{v}_e||^2_{[L^2(e)]^2} \le C \left(||\mathbf{u}_h - \mathbf{u}||^2_{[H^1(\Omega)]^2} + ||\boldsymbol{\xi}_{\tilde{h}} - \boldsymbol{\xi}||^2_{[H^{1/2}_{00}(\Gamma_N)]^2} \right). \qquad (2.23)$$

To bound the term involving the residual in the Neumann boundary condition, $\mathbf{g} - \boldsymbol{\sigma}_h \mathbf{n}$, we recall from the proof of Lemma 6.5 in [12] that

$$||(\boldsymbol{\sigma} - \boldsymbol{\sigma}_h)\mathbf{n}||_{[L^2(e)]^2} \le C\, h_e^{1/2} \Big(||\mathbf{div}(\boldsymbol{\sigma} - \boldsymbol{\sigma}_h)||_{[L^2(T)]^2} + c\, h_T^{-1} ||\boldsymbol{\sigma} - \boldsymbol{\sigma}_h||_{[L^2(T)]^2} \Big).$$

Then, multiplying by $\tilde{h}_e^{1/2}$ and using that $h_e \le \tilde{h}_e \le \tilde{h} \le C\,h$ and $C\,\tilde{h}_e \le C\,h \le h_e \le h_T$, we get

$$\begin{aligned} \sum_{e\in E(T)\cap E_h(\Gamma_N)} \tilde{h}_e\,||\mathbf{g} - \boldsymbol{\sigma}_h\mathbf{n}||^2_{[L^2(e)]^2} \;\le \\ \le\; C \sum_{e\in E(T)\cap E_h(\Gamma_N)} \Big(h_T^2\,||\mathbf{div}(\boldsymbol{\sigma} - \boldsymbol{\sigma}_h)||^2_{[L^2(T)]^2} \,+\, ||\boldsymbol{\sigma} - \boldsymbol{\sigma}_h||^2_{[L^2(T)]^2} \Big). \end{aligned} \tag{2.24}$$

Using inequalities (2.23) and (2.24), and the same techniques as in [8] with the remaining terms in (2.13), we deduce the efficiency of the a posteriori error estimator θ.

3 Non-homogeneous Dirichlet boundary conditions

In this section, we obtain an a posteriori error estimator of residual type for the augmented mixed finite element scheme introduced in [18] for the problem of linear elasticity with non-homogeneous Dirichlet boundary conditions. Given a volume force $\mathbf{f} \in [L^2(\Omega)]^2$ and a Dirichlet datum $\mathbf{g} \in [H^{1/2}(\Gamma)]^2$, we now consider the problem of determining the displacement $\mathbf{u}$ and the symmetric stress tensor $\boldsymbol{\sigma}$ of a linear elastic material occupying the region Ω:

$$\left\{ \begin{array}{rcll} \boldsymbol{\sigma} & = & \mathcal{C}\,\boldsymbol{\varepsilon}(\mathbf{u}) & \text{in } \Omega \\ -\mathbf{div}(\boldsymbol{\sigma}) & = & \mathbf{f} & \text{in } \Omega \\ \mathbf{u} & = & \mathbf{g} & \text{on } \Gamma \end{array} \right. \tag{3.1}$$

In the next two subsections, we recall the augmented variational and discrete formulations proposed in [18] to solve problem (3.1).

3.1 The augmented variational formulation

Let κ_1, κ_2, κ_3 and κ_4 be positive parameters independent of λ. The augmented variational formulation proposed in [18] for problem problem (3.1) reads: find $(\boldsymbol{\sigma}, \mathbf{u}, \boldsymbol{\gamma}) \in \mathbf{H}_0 := \tilde{H}_0 \times [H^1(\Omega)]^2 \times [L^2(\Omega)]^{2\times 2}_{\mathtt{skew}}$ such that

$$\tilde{A}((\boldsymbol{\sigma}, \mathbf{u}, \boldsymbol{\gamma}), (\boldsymbol{\tau}, \mathbf{v}, \boldsymbol{\eta})) \,=\, \tilde{F}(\boldsymbol{\tau}, \mathbf{v}, \boldsymbol{\eta}) \qquad \forall\,(\boldsymbol{\tau}, \mathbf{v}, \boldsymbol{\eta}) \in \mathbf{H}_0\,, \tag{3.2}$$

where $\tilde{H}_0 := \{\boldsymbol{\tau} \in H(\mathbf{div};\Omega) \,:\, \int_\Omega \mathrm{tr}(\boldsymbol{\tau}) \,=\, 0\}$, and the bilinear form $\tilde{A} : \mathbf{H}_0 \times \mathbf{H}_0 \to \mathbb{R}$ and the functional $\tilde{F} : \mathbf{H}_0 \to \mathbb{R}$ are given by

$$\tilde{A}((\boldsymbol{\sigma}, \mathbf{u}, \boldsymbol{\gamma}), (\boldsymbol{\tau}, \mathbf{v}, \boldsymbol{\eta})) := A((\boldsymbol{\sigma}, \mathbf{u}, \boldsymbol{\gamma}), (\boldsymbol{\tau}, \mathbf{v}, \boldsymbol{\eta})) \,+\, \kappa_4 \int_\Gamma \mathbf{u}\cdot\mathbf{v}\,,$$

$$\tilde{F}(\boldsymbol{\tau}, \mathbf{v}, \boldsymbol{\eta}) \,:=\, F(\boldsymbol{\tau}, \mathbf{v}, \boldsymbol{\eta}) \,+\, \langle \boldsymbol{\tau}\,\mathbf{n}, \mathbf{g}\rangle_\Gamma \,+\, \kappa_4 \int_\Gamma \mathbf{g}\cdot\mathbf{v} \,+\, \kappa_1\, c_{\mathbf{g}} \int_\Gamma \mathbf{v}\cdot\mathbf{n}\,,$$

where $A(\cdot,\cdot)$ and $F(\cdot)$ are defined in (2.4) and (2.5), respectively. In addition, we denote by $\langle\cdot,\cdot\rangle_\Gamma$ the duality pairing between $[H^{-1/2}(\Gamma)]^2$ and $[H^{1/2}(\Gamma)]^2$ with respect to the $[L^2(\Gamma)]^2$-inner product and, given $\mathbf{w}$ defined on Γ, we denote $c_{\mathbf{w}} := \frac{1}{2\,|\Omega|}\int_\Gamma \mathbf{w}\cdot\mathbf{n}$.

The following properties and results concerning $\tilde{A}(\cdot,\cdot)$ and the augmented formulation (3.2) were stablished in [18, Theorem 3.2]. In what follows, κ_0 is a constant of a Korn-type inequality (see [18] for details).

Theorem 3.1 *Assume that* $(\kappa_1,\kappa_2,\kappa_3,\kappa_4)$ *is independent of* λ *and such that* $0<\kappa_1<2\,\mu$, $0<\kappa_2$, $0<\kappa_3<\left(\dfrac{\kappa_0}{1-\kappa_0}\right)\kappa_1$ *if* $\kappa_0<1$ *or* $\kappa_3>0$ *if* $\kappa_0\geq 1$, *and* $\kappa_4\geq\kappa_1+\kappa_3$. *Then, there exist positive constants,* $\tilde{M}$ *and* $\tilde{\alpha}$, *independent of* λ, *such that*

$$\begin{aligned} |\,\tilde{A}((\boldsymbol{\sigma},\mathbf{u},\boldsymbol{\gamma}),(\boldsymbol{\tau},\mathbf{v},\boldsymbol{\eta}))\,| \;&\leq\; \tilde{M}\;\|(\boldsymbol{\sigma},\mathbf{u},\boldsymbol{\gamma})\|_{\mathbf{H}_0}\,\|(\boldsymbol{\tau},\mathbf{v},\boldsymbol{\eta})\|_{\mathbf{H}_0} \\ \tilde{A}((\boldsymbol{\tau},\mathbf{v},\boldsymbol{\eta}),(\boldsymbol{\tau},\mathbf{v},\boldsymbol{\eta})) \;&\geq\; \tilde{\alpha}\;\|(\boldsymbol{\tau},\mathbf{v},\boldsymbol{\eta})\|_{\mathbf{H}_0}^2 \end{aligned} \tag{3.3}$$

for all $(\boldsymbol{\sigma},\mathbf{u},\boldsymbol{\gamma})$, $(\boldsymbol{\tau},\mathbf{v},\boldsymbol{\eta})\in\mathbf{H}_0$. *In particular, taking* $\kappa_1=\tilde{C}_1\,\mu$, *with any* $\tilde{C}_1\in]0,2[$, $\kappa_2=\frac{1}{\mu}\left(1-\frac{\kappa_1}{2\,\mu}\right)$, $\kappa_3=\tilde{C}_3\,\kappa_1$, *with any* $\tilde{C}_3\in]0,\frac{\kappa_0}{1-\kappa_0}[$ *if* $\kappa_0<1$, *or* $\kappa_3=\kappa_1$ *if* $\kappa_0\geq 1$, *and* $\kappa_4=\kappa_1+\kappa_3$, *yields* $\tilde{M}$ *and* $\tilde{\alpha}$ *depending only on* μ, $\dfrac{1}{\mu}$ *and* Ω. *Moreover, the augmented variational formulation* (3.2) *has a unique solution* $(\boldsymbol{\sigma},\mathbf{u},\boldsymbol{\gamma})\in\mathbf{H}_0$, *and there exists a positive constant* C, *independent of* λ, *such that*

$$\|(\boldsymbol{\sigma},\mathbf{u},\boldsymbol{\gamma})\|_{\mathbf{H}_0}\;\leq\;C\left(\|\mathbf{f}\|_{[L^2(\Omega)]^2}+\|\mathbf{g}\|_{[H^{1/2}(\Gamma)]^2}\right).$$

Finally, we recall from [18] that, since we are looking for $\boldsymbol{\sigma}\in\tilde{H}_0$, the solution to problem (3.2) satisfies the modified constitutive law $\boldsymbol{\sigma}=\mathcal{C}(\boldsymbol{\varepsilon}(\mathbf{u})-c_{\mathbf{g}}\,\mathbf{I})$ in Ω.

3.2 The augmented mixed finite element method

Given a finite element subspace $\mathbf{H}_{0,h}\subseteq\mathbf{H}_0$, the Galerkin scheme associated to (3.2) reads: find $(\boldsymbol{\sigma}_h,\mathbf{u}_h,\boldsymbol{\gamma}_h)\in\mathbf{H}_{0,h}$ such that

$$\tilde{A}((\boldsymbol{\sigma}_h,\mathbf{u}_h,\boldsymbol{\gamma}_h),(\boldsymbol{\tau}_h,\mathbf{v}_h,\boldsymbol{\eta}_h))\;=\;\tilde{F}(\boldsymbol{\tau}_h,\mathbf{v}_h,\boldsymbol{\eta}_h)\qquad\forall\,(\boldsymbol{\tau}_h,\mathbf{v}_h,\boldsymbol{\eta}_h)\in\mathbf{H}_{0,h}\,. \tag{3.4}$$

The following result is also established in [18].

Theorem 3.2 *Assume that the parameters* κ_1, κ_2, κ_3 *and* κ_4 *satisfy the assumptions of Theorem* 3.1 *and let* $\mathbf{H}_{0,h}$ *be any finite element subspace of* $\mathbf{H}_0$. *Then, the Galerkin scheme* (3.4) *has a unique solution* $(\boldsymbol{\sigma}_h,\mathbf{u}_h,\boldsymbol{\gamma}_h)\in\mathbf{H}_{0,h}$, *and there exist positive constants,* C *and* $\tilde{C}$, *independent of* h *and* λ, *such that*

$$\|(\boldsymbol{\sigma}_h,\mathbf{u}_h,\boldsymbol{\gamma}_h)\|_{\mathbf{H}_0}\;\leq\;C\left(\|\mathbf{f}\|_{[L^2(\Omega)]^2}\,+\,\|\mathbf{g}\|_{[H^{1/2}(\Gamma)]^2}\right),$$

$$\|(\boldsymbol{\sigma},\mathbf{u},\boldsymbol{\gamma})-(\boldsymbol{\sigma}_h,\mathbf{u}_h,\boldsymbol{\gamma}_h)\|_{\mathbf{H}_0}\;\leq\;\tilde{C}\inf_{(\boldsymbol{\tau}_h,\mathbf{v}_h,\boldsymbol{\eta}_h)\in\mathbf{H}_{0,h}}\|(\boldsymbol{\sigma},\mathbf{u},\boldsymbol{\gamma})-(\boldsymbol{\tau}_h,\mathbf{v}_h,\boldsymbol{\eta}_h)\|_{\mathbf{H}_0}\,.$$

Proof. See Theorem 4.1 in [18]. □

Let $H_h^{\boldsymbol{\sigma}}$ and $H_h^{\boldsymbol{\gamma}}$ be the finite element subspaces defined in (2.8) and (2.10), respectively, and define

$$H_{0,h}^{\boldsymbol{\sigma}} := \left\{ \boldsymbol{\tau}_h \in H_h^{\boldsymbol{\sigma}} : \int_\Omega \operatorname{tr}(\boldsymbol{\tau}_h) = 0 \right\},$$
$$H_h^{\mathbf{u}} := \left\{ \mathbf{v}_h \in [C(\bar{\Omega})]^2 : \mathbf{v}_h|_T \in [\mathcal{P}_1(T)]^2 \quad \forall T \in \mathcal{T}_h \right\}.$$

Then, the simplest finite element subspace $\mathbf{H}_{0,h}$ of $\mathbf{H}_0$ is given by

$$\mathbf{H}_{0,h} := H_{0,h}^{\boldsymbol{\sigma}} \times H_h^{\mathbf{u}} \times H_h^{\boldsymbol{\gamma}}. \tag{3.5}$$

The rate of convergence of the Galerkin scheme (3.4) when the specific finite element subspace (3.5) is used is stablished in Theorem 4.2 in [18].

3.3 Residual-based a posteriori error analysis

In this section we derive an a posteriori error estimator of residual type for the Galerkin scheme (3.4). We assume that the hypotheses of Theorem 3.2 are satisfied and let $(\boldsymbol{\sigma}_h, \mathbf{u}_h, \boldsymbol{\gamma}_h) \in \mathbf{H}_{0,h}$ be the unique solution to the discrete scheme (3.4). Then, for any triangle $T \in \mathcal{T}_h$, we define the error indicator $\tilde{\theta}_T$ as follows:

$$\begin{aligned}
\tilde{\theta}_T^2 &:= \|\mathbf{f} + \mathbf{div}(\boldsymbol{\sigma}_h)\|_{[L^2(T)]^2}^2 + \frac{1}{4}\|\boldsymbol{\sigma}_h - \boldsymbol{\sigma}_h^{\mathtt{t}}\|_{[L^2(T)]^{2\times 2}}^2 + \|\boldsymbol{\gamma}_h - \frac{\nabla \mathbf{u}_h - (\nabla \mathbf{u}_h)^{\mathtt{t}}}{2}\|_{[L^2(T)]^{2\times 2}}^2 \\
&+ h_T^2 \Big(\|\mathbf{curl}(\mathcal{C}^{-1}\boldsymbol{\sigma}_h - \nabla \mathbf{u}_h + \boldsymbol{\gamma}_h)\|_{[L^2(T)]^2}^2 + \|\mathbf{curl}(\mathcal{C}^{-1}(\boldsymbol{\varepsilon}(\mathbf{u}_h) - \mathcal{C}^{-1}\boldsymbol{\sigma}_h))\|_{[L^2(T)]^2}^2 \Big) \\
&+ \sum_{e \in E(T)} h_e \|J[(\mathcal{C}^{-1}\boldsymbol{\sigma}_h - \nabla \mathbf{u}_h + \boldsymbol{\gamma}_h + c_{\mathbf{g}}\,\mathbf{I})\mathbf{t}_T]\|_{[L^2(e)]^2}^2 \\
&+ \sum_{e \in E(T)} h_e \|J[(\mathcal{C}^{-1}(\boldsymbol{\varepsilon}(\mathbf{u}_h) - \mathcal{C}^{-1}\boldsymbol{\sigma}_h - c_{\mathbf{u}_h}\,\mathbf{I}))\mathbf{t}_T]\|_{[L^2(e)]^2}^2 \\
&+ h_T^2 \Big(\|\mathbf{div}(\boldsymbol{\varepsilon}(\mathbf{u}_h) - \mathcal{C}^{-1}(\frac{\boldsymbol{\sigma}_h + \boldsymbol{\sigma}_h^{\mathtt{t}}}{2}))\|_{[L^2(T)]^2}^2 + \|\mathbf{div}(\boldsymbol{\gamma}_h - \frac{\nabla \mathbf{u}_h - (\nabla \mathbf{u}_h)^{\mathtt{t}}}{2})\|_{[L^2(T)]^2}^2 \Big) \\
&+ \sum_{e \in E(T)} h_e \|J[(\boldsymbol{\varepsilon}(\mathbf{u}_h) - \mathcal{C}^{-1}(\frac{\boldsymbol{\sigma}_h + \boldsymbol{\sigma}_h^{\mathtt{t}}}{2}) - c_{\mathbf{g}}\,\mathbf{I})\mathbf{n}_T]\|_{[L^2(e)]^2}^2 \\
&+ \sum_{e \in E(T)} h_e \|J[(\boldsymbol{\gamma}_h - \frac{1}{2}(\nabla \mathbf{u}_h - (\nabla \mathbf{u}_h)^{\mathtt{t}}))\mathbf{n}_T]\|_{[L^2(e)]^2}^2 \\
&+ \sum_{e \in E(T) \cap E_h(\Gamma)} h_e \Big(||\mathbf{g} - \mathbf{u}_h||_{[L^2(e)]^2}^2 + \left\| \frac{\partial}{\partial \mathbf{t}_T}(\mathbf{g} - \mathbf{u}_h) \right\|_{[L^2(e)]^2}^2 \Big).
\end{aligned} \tag{3.6}$$

We remark that if $\mathbf{g} = \mathbf{0}$ on Γ, the a posteriori error estimator $\tilde{\theta}_T$ does not coincide necessarily with the a posteriori error estimator obtained in [8] because in this case $\mathbf{u}_h$

may not live in $[H_0^1(\Omega)]^2$. On the other hand, the residual character of each term on the right hand side of (3.6) is clear. As usual, the expression $\tilde{\theta} := \left(\sum_{T\in\mathcal{T}_h} \tilde{\theta}_T^2\right)^{1/2}$ is employed as the global residual error estimator. In the following theorem we establish the reliability and efficiency of $\tilde{\theta}$.

Theorem 3.3 *Let $(\boldsymbol{\sigma}, \mathbf{u}, \boldsymbol{\gamma}) \in \mathbf{H}_0$ and $(\boldsymbol{\sigma}_h, \mathbf{u}_h, \boldsymbol{\gamma}_h) \in \mathbf{H}_{0,h}$ be the unique solutions to problems* (3.2) *and* (3.4)*, respectively, and assume that $\mathbf{g} \in [H^1(\Gamma)]^2$. Then, there exist positive constants, $C_{\mathtt{eff}}$ and $C_{\mathtt{rel}}$, independent of h and λ, such that*

$$C_{\mathtt{eff}}\,\tilde{\theta} \,\leq\, \|(\boldsymbol{\sigma} - \boldsymbol{\sigma}_h, \mathbf{u} - \mathbf{u}_h, \boldsymbol{\gamma} - \boldsymbol{\gamma}_h)\|_{\mathbf{H}_0} \,\leq\, C_{\mathtt{rel}}\,\tilde{\theta}\,. \tag{3.7}$$

The proof of Theorem 3.3 is similar to that of Theorem 2.2. We give a sketch of the proof in the next two subsections.

3.3.1 Reliability

In this case, we consider the unique solution $(\mathbf{z}, \boldsymbol{\sigma}^*) \in [H_0^1(\Omega)]^2 \times \tilde{H}_0$ to the boundary value problem

$$\left\{\begin{array}{rcll} \boldsymbol{\sigma}^* &=& \boldsymbol{\varepsilon}(\mathbf{z}) & \text{in } \Omega \\ -\mathbf{div}(\boldsymbol{\sigma}^*) &=& \mathbf{f} + \mathbf{div}(\boldsymbol{\sigma}_h) & \text{in } \Omega \\ \mathbf{z} &=& \mathbf{0} & \text{on } \Gamma\,. \end{array}\right.$$

The corresponding continuous dependence result implies that

$$||\boldsymbol{\sigma}^*||_{H(\mathbf{div};\,\Omega)} \,\leq\, C\,||\mathbf{f} + \mathbf{div}(\boldsymbol{\sigma}_h)||_{[L^2(\Omega)]^2} \tag{3.8}$$

with $C > 0$, independent of λ. Then, we proceed similarly as in subsection 2.3.1 and use that $\tilde{A}(\cdot,\cdot)$ is coercive and bounded in $\mathbf{H}_0$ to obtain that

$$\tilde{\alpha}\,||(\boldsymbol{\sigma} - \boldsymbol{\sigma}_h - \boldsymbol{\sigma}^*, \mathbf{u} - \mathbf{u}_h, \boldsymbol{\gamma} - \boldsymbol{\gamma}_h)||_{\mathbf{H}_0} \,\leq$$

$$\leq \sup_{\substack{(\boldsymbol{\tau},\mathbf{v},\boldsymbol{\eta})\in\mathbf{H}_0 \\ (\boldsymbol{\tau},\mathbf{v},\boldsymbol{\eta})\neq\mathbf{0} \\ \mathbf{div}(\boldsymbol{\tau})=\mathbf{0}}} \frac{|\tilde{A}((\boldsymbol{\sigma} - \boldsymbol{\sigma}_h, \mathbf{u} - \mathbf{u}_h, \boldsymbol{\gamma} - \boldsymbol{\gamma}_h), (\boldsymbol{\tau}, \mathbf{v}, \boldsymbol{\eta}))|}{||(\boldsymbol{\tau}, \mathbf{v}, \boldsymbol{\eta})||_{\mathbf{H}_0}} \,+\, \tilde{M}\,||\boldsymbol{\sigma}^*||_{H(\mathbf{div};\,\Omega)}. \tag{3.9}$$

To bound the first term on the right hand side of (3.9), we let $(\boldsymbol{\tau}, \mathbf{v}, \boldsymbol{\eta}) \in \mathbf{H}_0 \setminus \{\mathbf{0}\}$ with $\mathbf{div}(\boldsymbol{\tau}) \,=\, \mathbf{0}$ in Ω, consider the stream function $\boldsymbol{\varphi} \in [H^1(\Omega)]^2$ such that $\int_\Omega \varphi_i = 0$ $(i = 1, 2)$ and $\boldsymbol{\tau} = \underline{\mathbf{curl}}(\boldsymbol{\varphi})$, and define $\boldsymbol{\varphi}_h$ and $\boldsymbol{\tau}_h$ as in (2.19). Then, since $H(\mathbf{div};\,\Omega) \,=\, \tilde{H}_0 \oplus \mathbb{R}\,\mathbf{I}$, we have that $\boldsymbol{\tau}_h \,=\, \boldsymbol{\tau}_{h,0} + d_h\,\mathbf{I}$, with $\boldsymbol{\tau}_{h,0} \in H_{0,h}^{\boldsymbol{\sigma}}$ and $d_h \,=\, \frac{\int_\Omega tr(\boldsymbol{\tau}_h)}{2|\Omega|} \in \mathbb{R}$. Using that

$(\boldsymbol{\sigma}, \mathbf{u}, \boldsymbol{\gamma})$ and $(\boldsymbol{\sigma}_h, \mathbf{u}_h, \boldsymbol{\gamma}_h)$ are the solutions to problems (3.2) and (3.4), respectively, it follows that

$$
\begin{aligned}
&\tilde{A}((\boldsymbol{\sigma}-\boldsymbol{\sigma}_h, \mathbf{u}-\mathbf{u}_h, \boldsymbol{\gamma}-\boldsymbol{\gamma}_h), (\boldsymbol{\tau}, \mathbf{v}, \boldsymbol{\eta})) \\
&\quad = \tilde{A}((\boldsymbol{\sigma}-\boldsymbol{\sigma}_h, \mathbf{u}-\mathbf{u}_h, \boldsymbol{\gamma}-\boldsymbol{\gamma}_h), (\boldsymbol{\tau}-\boldsymbol{\tau}_h, \mathbf{v}-\mathbf{v}_h, \boldsymbol{\eta})) \,+\, \kappa_1 \frac{d_h}{2(\lambda+\mu)} \int_\Gamma (\mathbf{g}-\mathbf{u}_h)\cdot\mathbf{n}
\end{aligned}
$$

where we choose $\mathbf{v}_h := (I_h(v_1), I_h(v_2)) \in H_h^{\mathbf{u}}$ and use the orthogonality between symmetric and skew-symmetric tensors to obtain

$$
\tilde{A}((\boldsymbol{\sigma}-\boldsymbol{\sigma}_h, \mathbf{u}-\mathbf{u}_h, \boldsymbol{\gamma}-\boldsymbol{\gamma}_h), (d_h\,\mathbf{I}, \mathbf{0}, \mathbf{0})) = \kappa_1 \frac{d_h}{2(\lambda+\mu)} \int_\Gamma (\mathbf{g}-\mathbf{u}_h)\cdot\mathbf{n}\,.
$$

Then, we use that $(\boldsymbol{\sigma}, \mathbf{u}, \boldsymbol{\gamma})$ is the solution to (3.2) and the definition of the form $\tilde{F}$ to get

$$
\begin{aligned}
&\tilde{A}((\boldsymbol{\sigma}-\boldsymbol{\sigma}_h, \mathbf{u}-\mathbf{u}_h, \boldsymbol{\gamma}-\boldsymbol{\gamma}_h), (\boldsymbol{\tau}, \mathbf{v}, \boldsymbol{\eta})) \\
&\quad = \int_\Omega \mathbf{f}\cdot(\mathbf{v}-\mathbf{v}_h) \,+\, \langle(\boldsymbol{\tau}-\boldsymbol{\tau}_h)\mathbf{n}, \mathbf{g}\rangle_\Gamma \,+\, \kappa_4 \int_\Gamma \mathbf{g}\cdot(\mathbf{v}-\mathbf{v}_h) \,+\, \kappa_1 c_{\mathbf{g}} \int_\Gamma (\mathbf{v}-\mathbf{v}_h)\cdot\mathbf{n} \\
&\quad - A((\boldsymbol{\sigma}_h, \mathbf{u}_h, \boldsymbol{\gamma}_h), (\boldsymbol{\tau}-\boldsymbol{\tau}_h, \mathbf{v}-\mathbf{v}_h, \boldsymbol{\eta})) \,+\, \kappa_1 \frac{d_h}{2(\lambda+\mu)} \int_\Gamma (\mathbf{g}-\mathbf{u}_h)\cdot\mathbf{n}\,.
\end{aligned}
$$

Integrating by parts and making some algebraic manipulations, we obtain that

$$
\begin{aligned}
&\tilde{A}((\boldsymbol{\sigma}-\boldsymbol{\sigma}_h, \mathbf{u}-\mathbf{u}_h, \boldsymbol{\gamma}-\boldsymbol{\gamma}_h), (\boldsymbol{\tau}, \mathbf{v}, \boldsymbol{\eta})) \,= \\
&\quad = \int_\Omega (\mathbf{f}+\mathbf{div}(\boldsymbol{\sigma}_h))\cdot(\mathbf{v}-\mathbf{v}_h) + \langle(\boldsymbol{\tau}-\boldsymbol{\tau}_h)\mathbf{n}, \mathbf{g}-\mathbf{u}_h\rangle_\Gamma + \kappa_4 \int_\Gamma (\mathbf{g}-\mathbf{u}_h)\cdot(\mathbf{v}-\mathbf{v}_h) \\
&\quad - \int_\Omega (\boldsymbol{\tau}-\boldsymbol{\tau}_h) : \Big(\big(\mathcal{C}^{-1}\boldsymbol{\sigma}_h - \nabla\mathbf{u}_h + \boldsymbol{\gamma}_h + c_{\mathbf{g}}\,\mathbf{I}\big) - \kappa_1\, \mathcal{C}^{-1}\big(\boldsymbol{\varepsilon}(\mathbf{u}_h) - \mathcal{C}^{-1}\boldsymbol{\sigma}_h - c_{\mathbf{u}_h}\,\mathbf{I}\big) \Big) \\
&\quad - \int_\Omega \nabla(\mathbf{v}-\mathbf{v}_h) : \Big(\kappa_1 \Big(\boldsymbol{\varepsilon}(\mathbf{u}_h) - \mathcal{C}^{-1}\big(\frac{\boldsymbol{\sigma}_h+\boldsymbol{\sigma}_h^{\mathtt{t}}}{2}\big) - c_{\mathbf{g}}\,\mathbf{I}\Big) + \kappa_3 \Big(\boldsymbol{\gamma}_h - \frac{\nabla\mathbf{u}_h - (\nabla\mathbf{u}_h)^{\mathtt{t}}}{2}\Big) \Big) \\
&\quad + \int_\Omega \boldsymbol{\eta} : \Big(\frac{\boldsymbol{\sigma}_h - \boldsymbol{\sigma}_h^{\mathtt{t}}}{2} - \kappa_3 \big(\boldsymbol{\gamma}_h - \frac{\nabla\mathbf{u}_h - (\nabla\mathbf{u}_h)^{\mathtt{t}}}{2}\big) \Big).
\end{aligned}
\tag{3.10}
$$

The rest of the proof consists in deriving suitable upper bounds for each one of the terms appearing on the right hand side of (3.10). We observe that the first and the last terms are identical to the corresponding ones in (2.20). The fourth and fifth terms on the right hand side of (3.10) are very similar to second and third terms on the right hand side of (2.20), and can be bounded with the techniques described in subsection 2.3.1. The second term on the right hand side of (3.10) is analogous to the corresponding one in (2.20). More precisely, assuming that $\mathbf{g} \in [H^1(\Gamma)]^2$ and proceeding as in subsection 2.3.1, we obtain that

$$
|\langle(\boldsymbol{\tau}-\boldsymbol{\tau}_h)\mathbf{n}, \mathbf{g}-\mathbf{u}_h\rangle_\Gamma| \,\leq\, C\Big(\sum_{T\in\mathcal{T}_h} \sum_{e\in E(T)\cap E_h(\Gamma)} h_e \left\| \frac{\partial}{\partial\,\mathbf{t}}(\mathbf{g}-\mathbf{u}_h) \right\|_{[L^2(e)]^2}^2 \Big)^{1/2} \|\boldsymbol{\tau}\|_{H(\mathbf{div};\Omega)}\,.
$$

Finally, the third term on the right hand side of (3.10) can be bounded applying the Cauchy-Schwarz inequality and Lemma 1.1, and using that the number of triangles in $\Delta(e)$ is bounded independently of h:

$$\left|\int_\Gamma (\mathbf{g}-\mathbf{u}_h)\cdot(\mathbf{v}-\mathbf{v}_h)\right| \le C\Big(\sum_{e\in E(T)\cap E(\Gamma)} h_e\,\|\mathbf{g}-\mathbf{u}_h\|^2_{[L^2(e)]^2}\Big)^{1/2}\|\mathbf{v}\|_{[H^1(\Omega)]^2}\,.$$

3.3.2 Efficiency

In order to prove the efficiency of the a posteriori error estimator $\tilde\theta$ (lower bound in (3.7)), we first observe that most of the terms involved in the definition of $\tilde\theta$ are identical or very similar to those appearing in the definition of θ (see (2.13)), so that they can be bounded from above using the same techniques. We only have to bound the last term on the right hand side of (3.6). Using the Dirichlet boundary condition and a trace theorem, we obtain

$$\sum_{e\in E(T)\cap E_h(\Gamma)} h_e\,\|\mathbf{g}-\mathbf{u}_h\|^2_{[L^2(e)]^2} \le c\,\|\mathbf{u}-\mathbf{u}_h\|^2_{[H^1(\Omega)]^2}\,.$$

On the other hand, the continuity of the tangential derivative and a trace theorem gives the existence of $C>0$, independent of h and λ, such that

$$\sum_{e\in E(T)\cap E_h(\Gamma)} h_e\,\left\|\frac{\partial}{\partial\mathbf{t}}(\mathbf{g}-\mathbf{u}_h)\right\|^2_{[L^2(e)]^2} \le C\,\|\mathbf{u}-\mathbf{u}_h\|^2_{[H^1(\Omega)]^2}$$

Proceeding with the remaining terms as indicated in subsection 2.3.2 (see also [8, 11, 12]), we deduce the lower bound in (3.7).

4 Numerical results

In this section we present several numerical results that illustrate the performance of the augmented mixed finite element schemes (2.7) and (3.4), and of the adaptive algorithms based on the a posteriori error estimators θ and $\tilde\theta$ analyzed in this paper. We use the simplest finite element subspaces described in subsections 2.3 and 3.3, respectively. The numerical experiments given below were obtained using a *Pentium Xeon* computer with dual processors and a Matlab code. The augmented mixed schemes (2.7) and (3.4) were implemented following the ideas explained in [17, section 4.3].

We recall that, given the Young modulus E and the Poisson ratio ν of a linear elastic material, the corresponding Lamé constants are defined by $\mu := \frac{E}{2(1+\nu)}$ and $\lambda := \frac{E\,\nu}{(1+\nu)\,(1-2\,\nu)}$. In the examples below, we fix $E = 1$ and consider the values $\nu = 0.4900$ and $\nu = 0.4999$, which yield the following values of μ and λ:

ν	μ	λ
0.4900	0.3356	16.4430
0.4999	0.3334	1666.4444

Given an error indicator η_T, for each $T \in \mathcal{T}_h$ we consider the following adaptive algorithm (see [25]):

1. Start with a coarse mesh $\mathcal{T}_h$.

2. Solve the Galerkin scheme for the current mesh $\mathcal{T}_h$.

3. Compute η_T for each triangle $T \in \mathcal{T}_h$.

4. Consider stopping criterion and decide to finish or go to the next step.

5. Refine each element $T' \in \mathcal{T}_h$ such that

$$\eta_{T'} \,\geq\, \frac{1}{2}\,\max\{\eta_T \,:\, T \in \mathcal{T}_h\}\,.$$

6. Define the resulting mesh as the new $\mathcal{T}_h$ and go to step 2.

In what follows, $\mathcal{N}$ stands for the total number of degrees of freedom (dof) of the corresponding augmented discrete scheme. We define the experimental rate of convergence as

$$r(e) \,:=\, -\,2\,\frac{\log(e/e')}{\log(\mathcal{N}/\mathcal{N}')}\,,$$

where $\mathcal{N}$ and $\mathcal{N}'$ denote the dof of two consecutive triangulations, and e and e' are the corresponding total errors.

4.1 Mixed boundary conditions

In this case, according to the compatibility condition required in Theorem 4.10 in [17], we choose as independent partition of the Neumann boundary the one obtained inserting a node between every two ones of the partition on Γ_N inherited from $\mathcal{T}_h$. In addition, we consider $\kappa_1 \,=\, \mu$, $\kappa_2 \,=\, \frac{1}{2\,\mu}$ and $\kappa_3 \,=\, \frac{\mu}{8}$, which corresponds to a feasible choice, as described in Theorem 2.1.

Let $(\boldsymbol{\sigma}, \mathbf{u}, \boldsymbol{\gamma}, \boldsymbol{\xi})$ and $(\boldsymbol{\sigma}_h, \mathbf{u}_h, \boldsymbol{\gamma}_h, \boldsymbol{\xi}_{\tilde{h}})$ be the unique solutions to the augmented and discrete variational formulations (2.3) and (2.7), respectively. We define the individual errors $e(\boldsymbol{\sigma}) := \|\boldsymbol{\sigma} - \boldsymbol{\sigma}_h\|_{H(\mathbf{div};\,\Omega)}$, $e(\mathbf{u}) := |\mathbf{u} - \mathbf{u}_h|_{[H^1(\Omega)]^2}$, $e(\boldsymbol{\gamma}) := \|\boldsymbol{\gamma} - \boldsymbol{\gamma}_h\|_{[L^2(\Omega)]^{2\times 2}}$ and $e(\boldsymbol{\xi}) := \|\boldsymbol{\xi} - \boldsymbol{\xi}_h\|_{[H^{1/2}_{00}(\Gamma_N)]^2}$ and the total error as

$$e_{\mathtt{total}} := \Big(\, e(\boldsymbol{\sigma})^2 \,+\, e(\mathbf{u})^2 \,+\, e(\boldsymbol{\gamma})^2 \,+\, e(\boldsymbol{\xi})^2 \,\Big)^{1/2}.$$

Then, the effectivity index with respect to θ is given by $e_{\mathtt{total}}/\theta$. The individual errors are computed on each triangle using a Gaussian quadrature rule.

In order to illustrate the performance of the adaptive algorithm based on θ, we consider examples 1 and 2 specified in the table below. In example 1, $\Gamma_D := \big(\{0\} \times [0,1]\big) \cup \big([0,1] \times \{0\}\big)$ and the solution has a singularity at the boundary point $(0,0)$. In fact, the behaviour of $\mathbf{u}$ in a neighborhood of the origin implies that $\mathbf{div}(\boldsymbol{\sigma}) \in [H^{2/3}(\Omega)]^2$ only, which according to Theorem 4.10 in [17] yields $2/3$ as the expected rate of convergence for the uniform refinement. In example 2, $\Gamma_D := \{\mathbf{x} := (x_1, x_2)^{\mathrm{t}} \in \mathbb{R}^2 \,:\, x_1^2 + x_2^2 = 1\}$ and the solution shows large stress regions in a neighborhood of the Dirichlet boundary Γ_D. In both cases, we take $\nu = 0.4900$ and choose the data $\mathbf{f}$ and $\mathbf{g}$ so that the exact solution is $\mathbf{u}(x_1, x_2) := (u_1(x_1, x_2), u_2(x_1, x_2))^{\mathtt{t}}$. Here, uniform refinement means that, given a uniform initial triangulation, each subsequent mesh is obtained from the previous one by bisecting each triangle by connecting the midpoint of its longest side with the opposed vertex. We use the *bisection procedure* as refinement algorithm.

Example	Ω	$\mathbf{u}(x_1, x_2)$
1	$]-1,1[^2 \setminus [0,1]^2$	$u_1(x_1, x_2) = u_2(x_1, x_2) = r^{5/3} \sin((2\theta - \pi)/3)$
2	$]0,2[^2 \setminus B[0,1]$	$\mathbf{u}(x_1, x_2) = 5(1 - x_1^2 - x_2^2) e^{-5(1-x_1^2-x_2^2)^2} (x_1, -x_2)^{\mathtt{t}}$

In Figures 4.1 and 4.3 we display the total error $e_{\mathtt{total}}$ versus the degrees of freedom $\mathcal{N}$ for the uniform and adaptive refinements for examples 1 and 2, respectively. We observe that the errors of the adaptive procedure decrease much faster than those obtained with the uniform one. In particular, in example 1 (where the experimental rate of convergence $r(e_{\mathtt{total}})$ approaches $2/3$ for the uniform refinement), the adaptive method is able to recover, at least approximately, the rate of convergence $\mathcal{O}(h)$ for the total error. Furthermore, the effectivity indexes are in a neighborhood of 0.5 for the uniform refinement and 0.25 for the adaptive refinement in example 1 (the corresponding values for example 2 are 0.57 and 0.61). In conclusion, they remain bounded from above and below, which confirms the reliability and efficiency of θ for the adaptive algorithm.

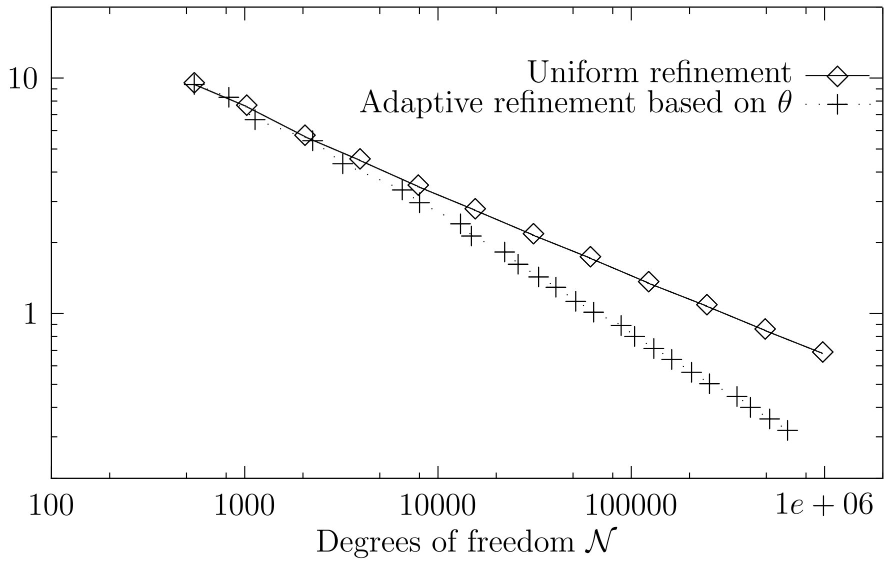

Figure 4.1: Ex. 1: Total error vs. dof, uniform and adaptive refinements.

Finally, some intermediate meshes obtained with the adaptive refinement procedure are displayed in Figures 4.2 and 4.4. We remark that the method is able to recognize the singularities and the large stress regions of the solutions. In particular, in example 1 (Figure 4.2) the adapted meshes are highly refined around the singular point $(0, 0)$. Similarly, the adapted meshes obtained in example 2 (Figure 4.4) concentrate the refinements around the Dirichlet boundary, where the largest stresses occur.

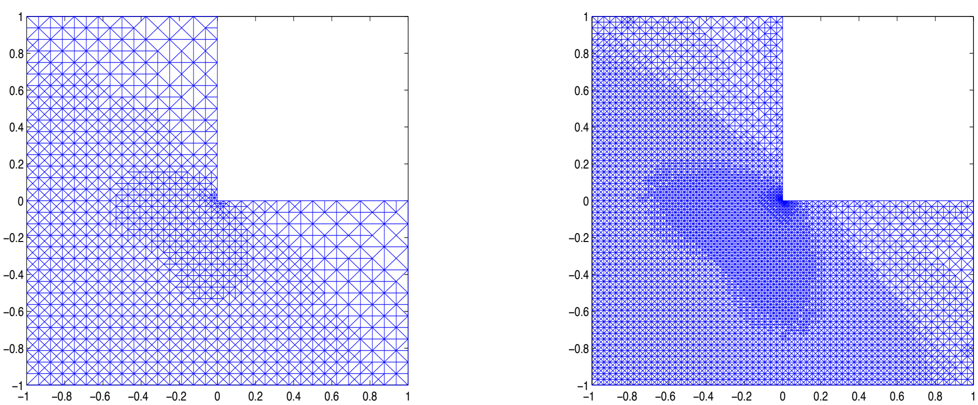

Figure 4.2: Ex. 1: adapted intermediate meshes with 15015 dof (left) and 64244 dof (right).

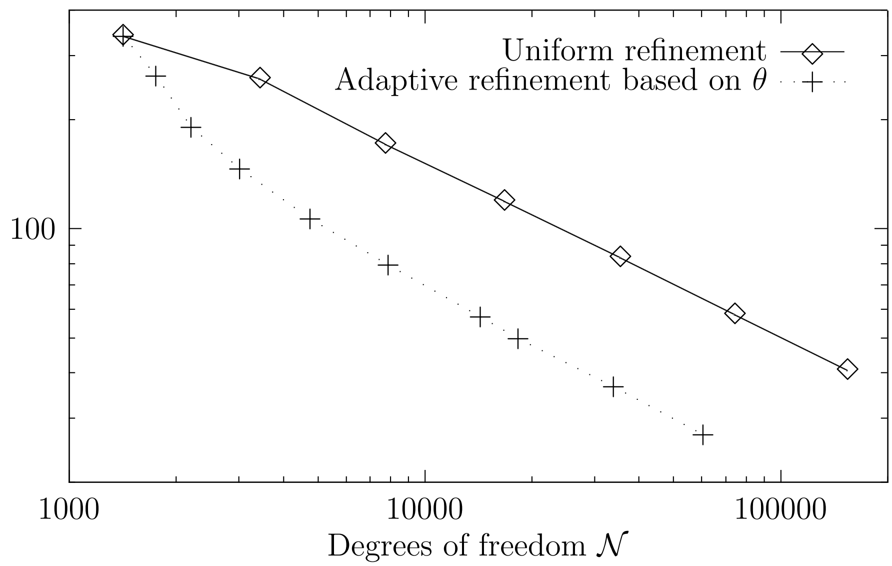

Figure 4.3: Ex. 2: Total error vs. dof, uniform and adaptive refinements.

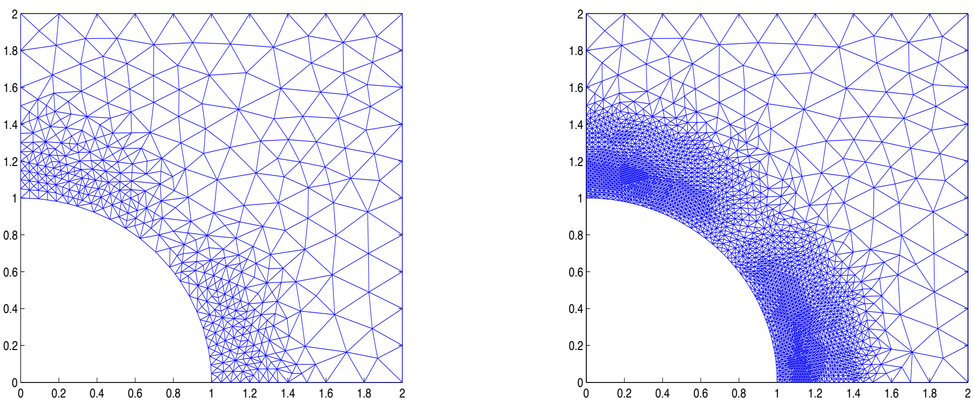

Figure 4.4: Ex. 2: adapted intermediate meshes with 4768 dof (left) and 33982 dof (right).

We end this section with some numerical results concerning the performance of the augmented mixed finite element scheme (2.7) and the adaptive algorithm based on θ as applied to approximate the solution of the classical Cook membrane problem. We let $\Omega := [0,48]\times[0,60]\setminus\{(x_1,x_2)\in\mathbb{R}^2/x_2<\frac{11x_1}{12}\ \ or\ \ x_2>\frac{x_1}{3}\}$, $\Gamma_D := \{(x_1,x_2)\in\bar{\Omega}/\ x_1=0\}$ and $\Gamma_N = \partial\Omega\setminus\bar{\Gamma}_D$. We assume $\mathbf{f}=\mathbf{0}$, $\mathbf{g}(x_1,x_2)=(0,1)^{\mathbf{t}}$ if $(x_1,x_2)\in\Gamma_N$ with $x_1=48$ and $\mathbf{g}=\mathbf{0}$ on the remaining part of Γ_N. The material parameters are $E=2900$ and $\nu=0.3$. Due to the equivalence between the a posteriori error estimator θ and the total error, we can use θ to show the convergence behavior for the uniform and adaptive refinements. In Figure 4.5 we observe that the errors of the adaptive procedure decrease much faster than those obtained with the uniform one. In this case, uniform refinement means that, given a uniform initial triangulation, each subsequent mesh is obtained from the previous one by dividing each triangle into the four ones arising when connecting the midpoints of its sides. We used an adaptive algorithm based on the *blue-green procedure* to refine the meshes (see [25] for more details).

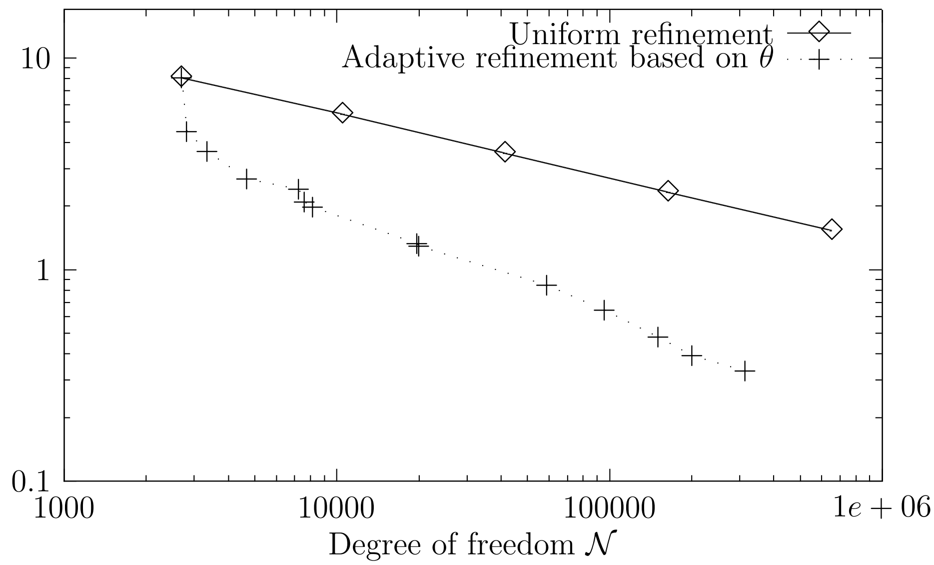

Figure 4.5: Cook membrane problem: θ vs. dof, uniform and adaptive refinements.

Some intermediates meshes obtained with the adaptive refinement are shown in Figure 4.6. The deformation is displayed with a magnification factor of 50. We remark that the algorithm is able to recognize the large stress regions of the solution.

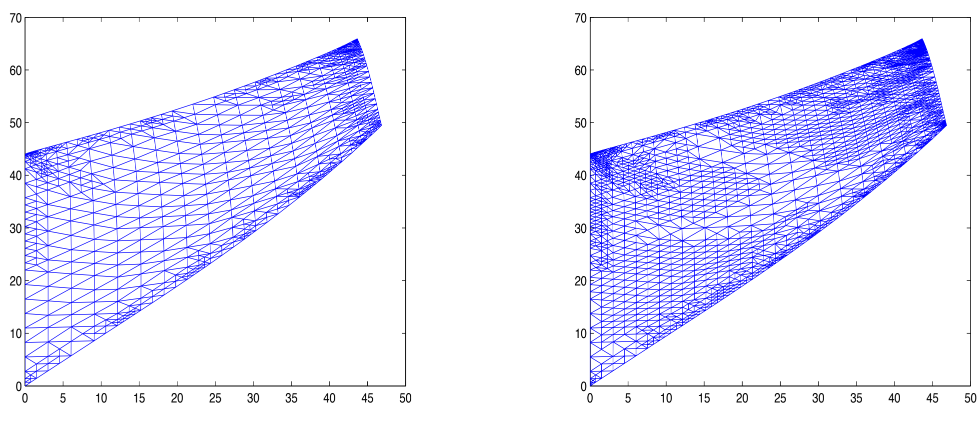

Figure 4.6: Cook membrane problem: adapted intermediate meshes with 7605 dof (left) and 19713 dof (right).

4.2 Pure displacement problem

In this section we present several numerical results that illustrate the performance of the augmented mixed finite element scheme (3.4) and the a posteriori error estimator $\tilde{\theta}$. We implemented the simplest finite element subspace $\mathbf{H}_{0,h}$ defined in (3.5). The zero mean condition on the traces of functions in $H_{0,h}^{\boldsymbol{\sigma}}$ is taken into account as described in section 4.3 of [17] (see also section 5 in [8]). According to Theorem 3.1, we consider the following values for the parameters κ_1, κ_2, κ_3 and κ_4:

$$\kappa_1 = \mu, \quad \kappa_2 = \frac{1}{2\,\mu}, \quad \kappa_3 = \frac{1}{8}\,\kappa_1, \quad \kappa_4 = \kappa_1 + \kappa_3.$$

Let $(\boldsymbol{\sigma}, \mathbf{u}, \boldsymbol{\gamma})$ and $(\boldsymbol{\sigma}_h, \mathbf{u}_h, \boldsymbol{\gamma}_h)$ be the unique solutions to the augmented variational and discrete problems (3.2) and (3.4), respectively. We use the same notations as in the previous subsection for the individual errors $e(\boldsymbol{\sigma})$ and $e(\boldsymbol{\gamma})$, and denote by $e(\mathbf{u}) := \|\mathbf{u} - \mathbf{u}_h\|_{[H^1(\Omega)]^2}$. The total error is given now by

$$e_{\texttt{total}} := \left(e(\boldsymbol{\sigma})^2 \,+\, e(\mathbf{u})^2 \,+\, e(\boldsymbol{\gamma})^2\right)^{1/2},$$

and the effectivity index with respect to $\tilde{\theta}$ is defined by $e_{\texttt{total}}/\tilde{\theta}$. Again, the individual errors are computed on each triangle using a Gaussian quadrature rule.

In order to illustrate the performance of the adaptive algorithm based on $\tilde{\theta}$, we consider three examples, specified in the table below. In example 3, the solution shows large stress regions in a neighborhood of the interior point $(0.7, 0.7)$. In example 4, the solution has a singularity at the boundary point $(0, 0)$. In fact, the behaviour of $\mathbf{u}$ in a neighborhood of the origin implies that $\mathbf{div}(\boldsymbol{\sigma}) \in [H^{1/3}(\Omega)]^2$, which according to Theorem 4.2 in [18], yields $1/3$ as the expected rate of convergence for the uniform refinement. Finally, the solution of example 5 shows large stress regions around the curved line $x_1^2 + x_2^2 = 0.1^2$. In all cases, we take $\nu = 0.4900$ and choose the data $\mathbf{f}$ and $\mathbf{g}$ so that the exact solution is $\mathbf{u}(x_1, x_2) := (u_1(x_1, x_2), u_2(x_1, x_2))^{\texttt{t}}$. In this case, we use the *blue-green procedure* to refine the meshes.

Example	Ω	$u_1(x_1, x_2) \,=\, u_2(x_1, x_2)$
3	$]0, 1[^2$	$\dfrac{1}{100[(x_1 - 0.7)^2 + (x_2 - 0.7)^2] + 1}$
4	$]-0.25, 0.25[^2 \backslash [0, 0.25]^2$	$\dfrac{x_1\,x_2}{(x_1^2 + x_2^2)^{1/3}} + 3x_1$
5	$]0, 1[^2 \backslash \{\mathbf{x} \in \mathbb{R}^2 : \, \|\mathbf{x}\| \le 0.1\}$	$\dfrac{10^{-4}}{x_1^2 + x_2^2 - 0.09^2}$

In Figures 4.7, 4.9 and 4.11 we display the total error $e_{\texttt{total}}$ versus the degrees of freedom $\mathcal{N}$ for the uniform and adaptive refinements for examples 3, 4 and 5, respectively.

In this case, uniform refinement means that, given a uniform initial triangulation, each subsequent mesh is obtained from the previous one by dividing each triangle into the four ones arising when connecting the midpoints of its sides. We observe from these figures that the errors of the adaptive procedure decrease much faster than those obtained by the uniform one. Furthermore, we observed that the effectivity indexes remain bounded from above and below. More precisely, the values of the effectivity index in example 3 are in a neighborhood of 0.7 for the uniform refinement and 0.8 for the adaptive refinement; the corresponding values for example 4 are 0.9 for the uniform refinement and 0.84 for the adaptive one; for example 5, the effectivity index is about 0.99 for both the uniform and the adaptive refinements. These results confirm the reliability and efficiency of the a posteriori error estimator $\tilde{\theta}$.

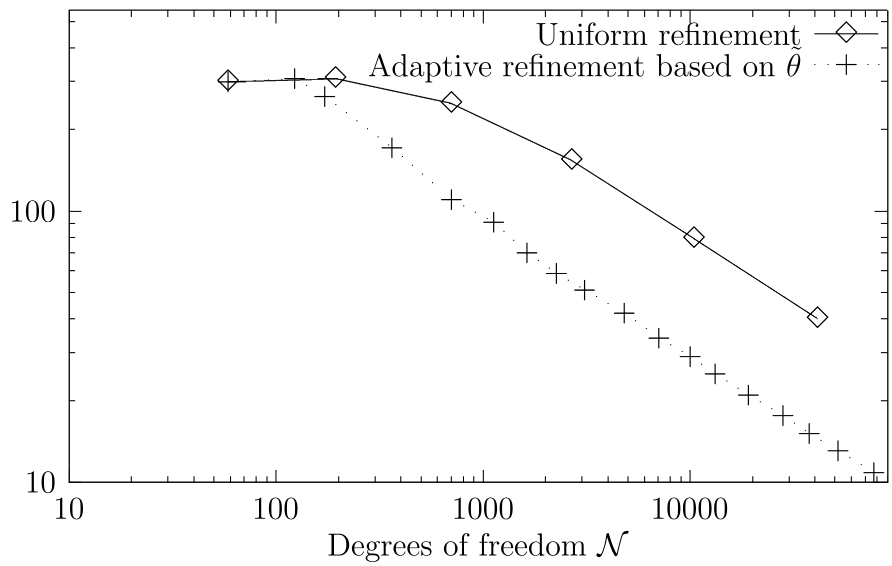

Figure 4.7: Ex. 3: Total error vs. dof, uniform and adaptive refinements.

Finally, some intermediates meshes obtained with the adaptive refinement are displayed in Figures 4.8, 4.10 and 4.12. We remark that the algorithm is able to recognize the singularities and large stress regions of the solutions.

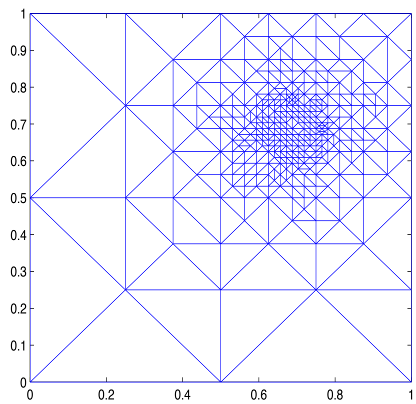

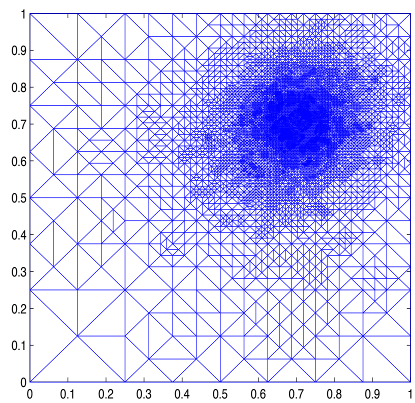

Figure 4.8: Ex. 3: adapted intermediate meshes with 3095 dof (left) and 77312 (right).

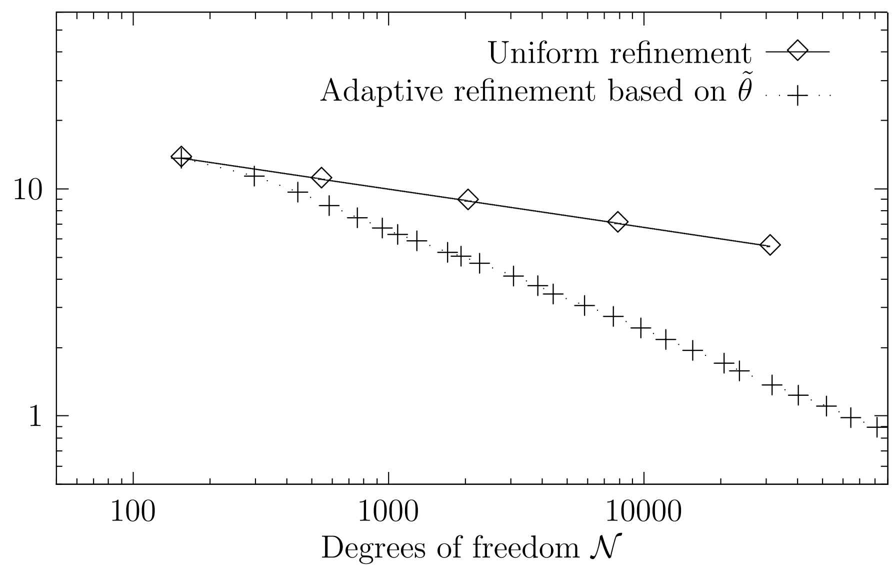

Figure 4.9: Ex. 4: Total error vs. dof, uniform and adaptive refinements.

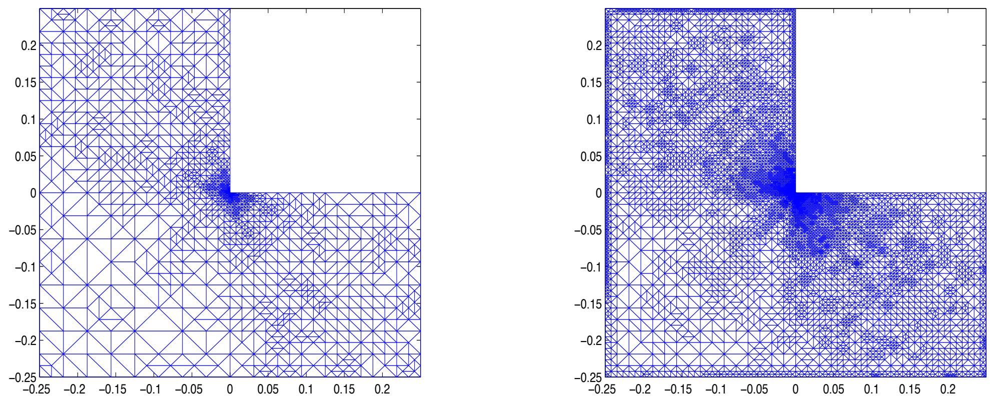

Figure 4.10: Ex. 4: adapted intermediate meshes with 15567 dof (left) and 81989 dof (right).

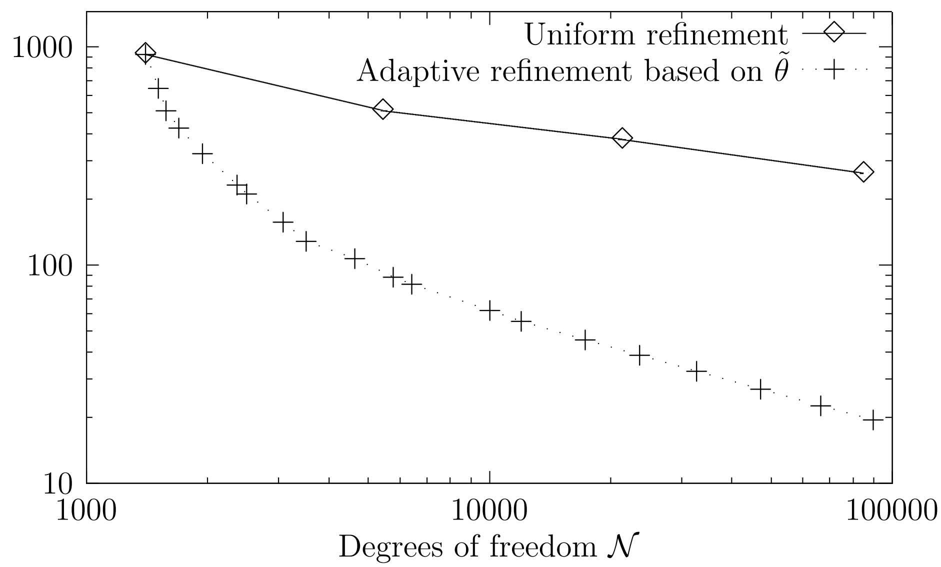

Figure 4.11: Ex. 5: Total error vs. dof, uniform and adaptive refinements.

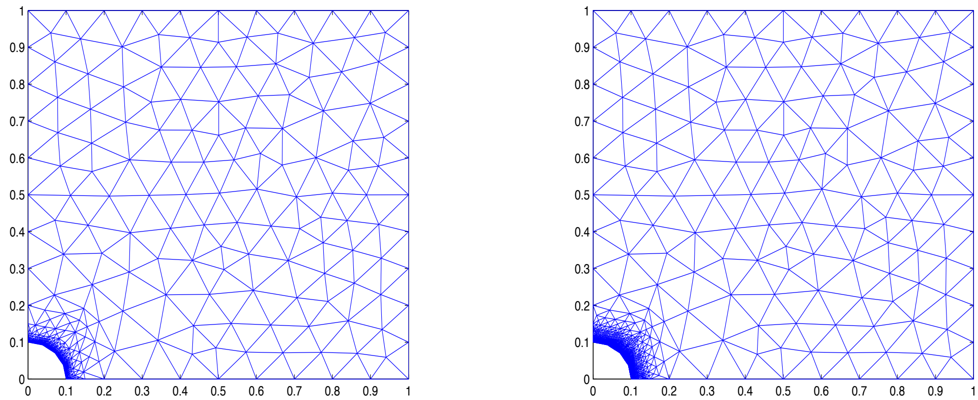

Figure 4.12: Ex. 5: adapted intermediate meshes with 17329 dof (left) and 89938 dof (right).

In summary, the numerical results presented in this section underline the reliability and efficiency of the error estimators θ and $\tilde{\theta}$, and strongly demonstrate that the associated adaptive algorithms are much more suitable than a uniform discretization procedure when solving problems with non-smooth solutions.

References

[1] D.N. Arnold, F. Brezzi and J. Douglas, *PEERS: A new mixed finite element method for plane elasticity*. Japan Journal of Applied Mathematics, vol. 1, pp. 347-367, (1984).

[2] D.N. Arnold, R.S. Falk and R. Winther, *Differential complexes and stability of finite element methods II. The elasticity complex*. In *Compatible spatial discretizations*, D.N. Arnold, P. Bochev, R. Leoucq, R. Nicolaides and M. Shashkov, eds., IMA Volumes in Mathematics and its Applications 142, Springer-Verlag 2005, 23-46.

[3] D.N. Arnold, R.S. Falk and R. Winther, *Finite element exterior calculus, homological techniques and applications*. Acta Numerica (2006), pp. 1-155.

[4] D.N. Arnold, R.S. Falk and R. Winther, *Mixed finite element methods for linear elasticity with weakly imposed symmetry*. Math. Comp., vol. 76, 260, pp. 1699-1723, (2007).

[5] D.N. Arnold and R. Winther, *Mixed finite elements for elasticity*. Numer. Math., vol. 92, pp. 401-419, (2002).

[6] I. Babuška and G.N. Gatica, *On the mixed finite element method with Lagrange multipliers*. Numerical Methods for Partial Differential Equations, vol. 19, 2, pp.192-210, (2003).

[7] T.P. Barrios and G.N. Gatica, *An augmented mixed finite element method with Lagrange multipliers: A priori and a posteriori error analyses*, J. Comp. Appl. Math., vol. 200, 2, pp. 653-676, (2007).

[8] T.P. Barrios, G.N. Gatica, M. González and N. Heuer, *A residual based a posteriori error estimator for an augmented mixed finite element method in linear elasticity*, M2AN Math. Model. Numer. Anal., vol. 40, 5, pp. 843-869, (2006).

[9] F. Brezzi and M. Fortin, Mixed and Hybrid Finite Element Methods. Springer Verlag, 1991.

[10] C. Carstensen, *An a posteriori error estimate for a first-kind integral equation*. Mathematics of Computation, vol. 66, 217, pp. 139-155, (1997).

[11] C. Carstensen, *A posteriori error estimate for the mixed finite element method*. Mathematics of Computation, vol. 66, 218, pp. 465-476, (1997).

[12] C. Carstensen and G. Dolzmann, *A posteriori error estimates for mixed FEM in elasticity*. Numer. Math., vol. 81, pp. 187-209, (1998).

[13] C. Carstensen, D. Günther, J. Reininghaus and J. Thiele, *The Arnold-Winther mixed FEM in linear elasticity. Part I: Implementation and numerical verification*. Comput. Methods Appl. Mech. Engrg., vol. 197, pp. 3014-3023, (2008).

[14] P.G. Ciarlet, The Finite Element Method for Elliptic Problems. North-Holland, 1978.

[15] P. Clément, *Approximation by finite element functions using local regularisation*. RAIRO Modélisation Mathématique et Analyse Numérique, vol. 9, pp. 77-84, (1975).

[16] G.N. Gatica, *A note on the efficiency of residual-based a-posteriori error estimators for some mixed finite element methods*. Electron. Trans. Numer. Anal., vol. 17, pp. 218-233, (2004).

[17] G.N. Gatica, *Analysis of a new augmented mixed finite element method for linear elasticity allowing $\mathbb{RT}_0$-$\mathbb{P}_1$-$\mathbb{P}_0$ approximations*. M2AN Math. Model. Numer. Anal., vol. 40, 1, pp. 1-28, (2006).

[18] G.N. Gatica, *An augmented mixed finite element method for linear elasticity with non-homogeneous Dirichlet conditions*. Electron. Trans. Numer. Anal. 26 (2007), 421–438.

[19] G.N. Gatica, Private Communication (2009).

[20] G.N. Gatica, A. Márquez and S. Meddahi, *An augmented mixed finite element method for 3D linear elasticity problems*. J. Comput. Appl. Math., vol. 231, pp. 526-540, (2009).

[21] G.N. Gatica, R. Oyarzúa and F.-J. Sayas, *Analysis of fully-mixed finite element methods for the Stokes-Darcy coupled problem*. Preprint 2009-08, Departamento de Ingeniería Matemática, Universidad de Concepción, Chile (2009).

[22] J.-L. Lions and E. Magenes, *Problemas aux Limites non Homogenes et Applications I*, Dunod, Paris, 1968.

[23] R. Stenberg, *A family of mixed finite elements for the elasticity problem*. Numerische Mathematik, vol. 53, 5, pp. 513-538, (1988).

[24] R. Verfürth, *A posteriori error estimation and adaptive mesh-refinement techniques*. Journal of Computational and Applied Mathematics, vol. 50, pp. 67-83, (1994).

[25] R. Verfürth, A Review of A Posteriori Error Estimation and Adaptive Mesh-Refinement Techniques. Wiley-Teubner (Chichester), 1996.

[26] R. Verfürth, *A review of a posteriori error estimation techniques for elasticity problems*, Comp. Meth. Appl. Mech. Engng. 176 (1-4), pp. 419-440, (1999).